

1. Femtosecond Laser Microprocessing
of Biomaterials

2. Nonlinear Optics of Nanoparticles
and their Application in Biomedicine

Dr. Vladimir Hovhannisyan

*Department of Physics,
Taiwan National University, Taipei*

Application femtosecond lasers

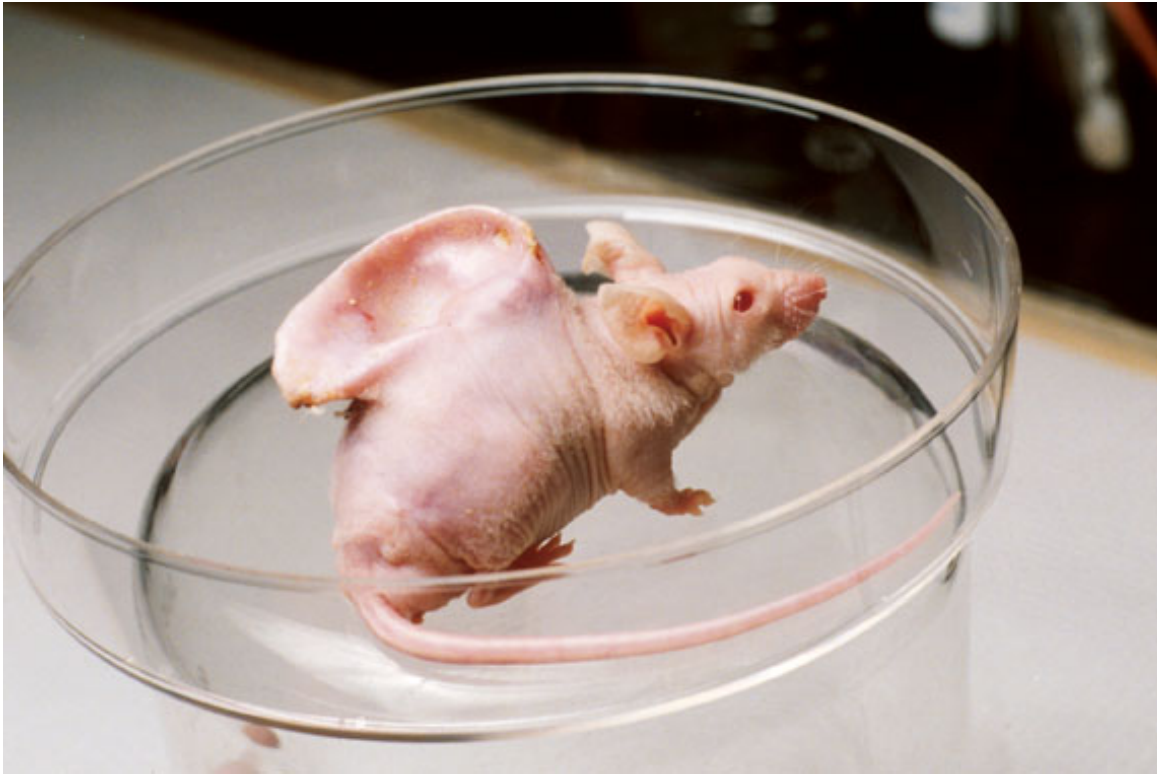
Near infrared **femtosecond (FS) lasers** are promising tools for minimally invasive tissue surgery and **scaffold** fabrication for **tissue engineering**.

The performance of FS laser **photomodification** proved to be **precise, repeatable** and **predictable**.

In addition, FS lasers enable novel nonlinear optical imaging, like **second harmonic generation (SHG)** and **two photon excited fluorescence (TPF) microscopy**.

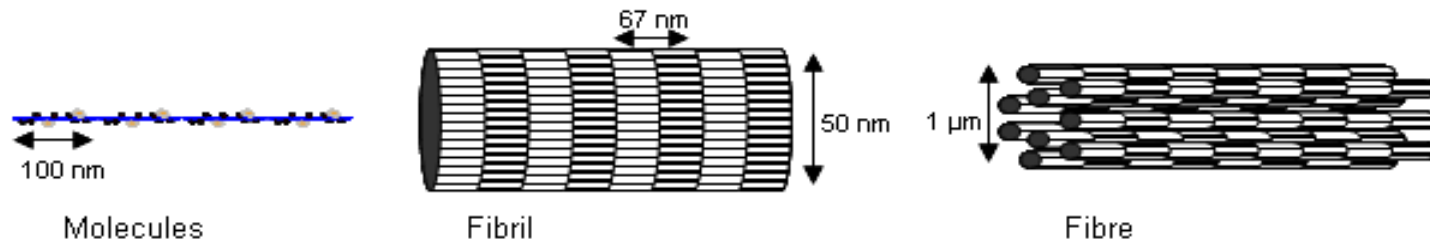
Tissue engineering and regenerative medicine.

Tissue engineering is a new scientific field aimed to create living, functional tissues for replacing damaged tissue or organ.



Fabrication of **3D scaffolds** with the desired microarchitecture from **collagen** or/and other natural materials is a challenge in tissue engineering and **regenerative medicine**.

Collagen

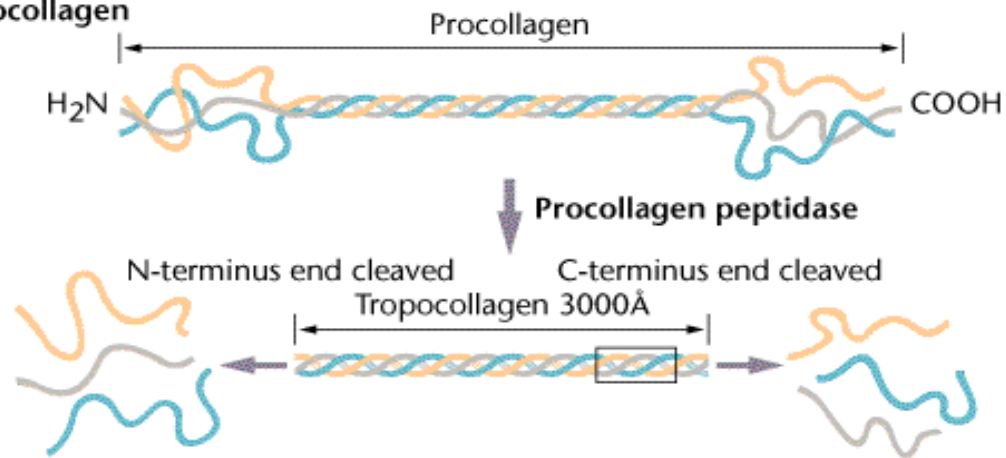


Col is the main protein of connective tissues and the most abundant protein in mammals (~25%). Col structural organization is responsible for biomechanical properties and specific functions of the connective tissues.

Col is composed of 3 alpha chains consisted of the regularly arranged amino acids, which are the basic units for collagen sub-units: Gly-X-Y. Gly stands for glycine, and X and Y represent any combination of other amino acid residues with 9% being proline and hydroxyproline. Derivatives of lysine and proline play important roles in the stabilization of globular structure and the shape of the fiber by forming covalent bonds.

Each chain contains precisely 1050 amino acids, and curls around with one another in a characteristic fashion of right-handed triple helix. Molecular weight-300000D

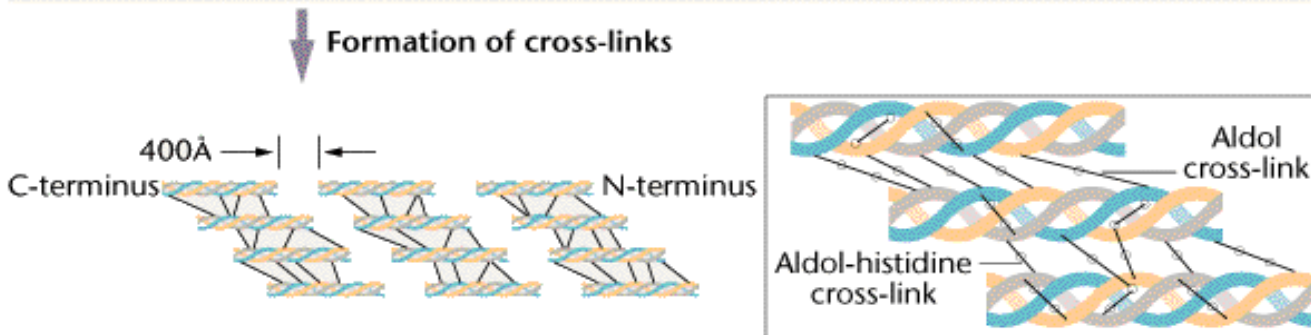
(a) Formation of tropocollagen



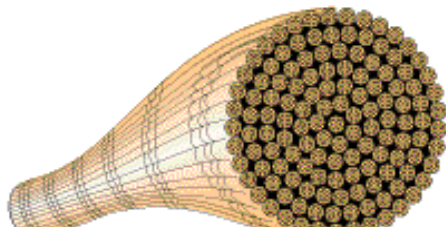
(b) Association of tropocollagen into collagen fiber



Formation of cross-links

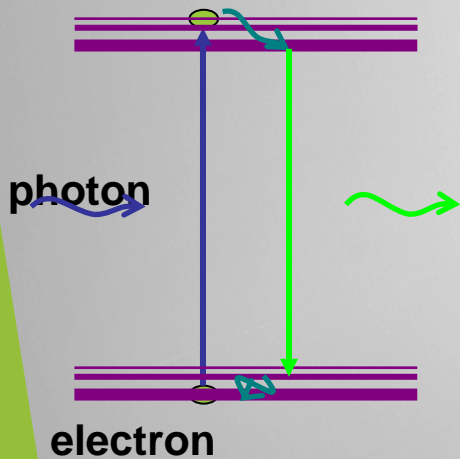
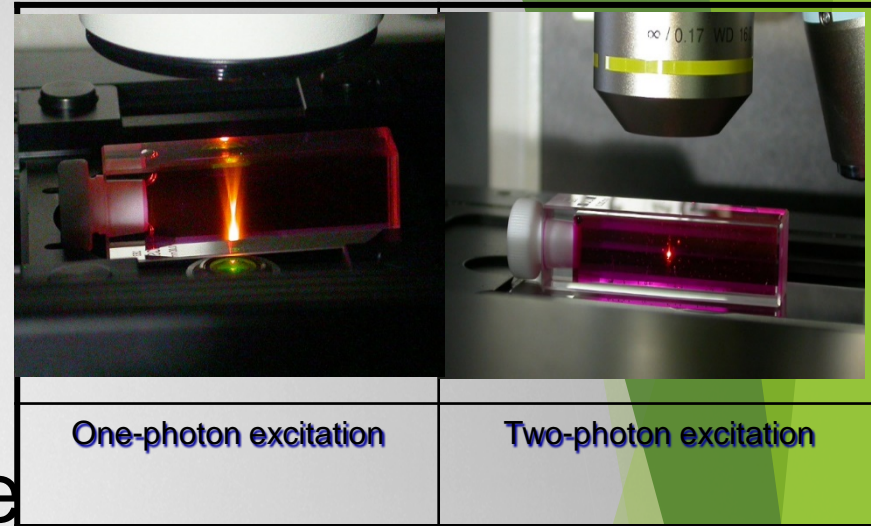


(Klug & Cummings 1997)

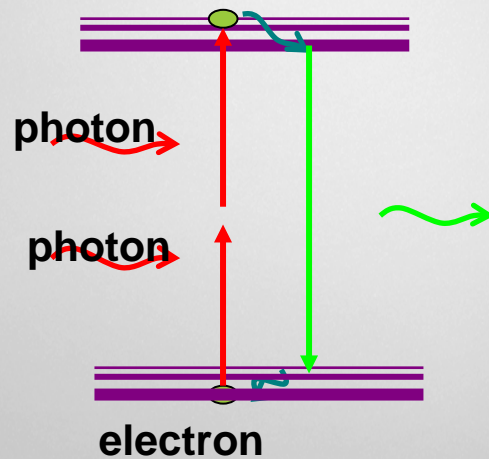


Non-linear Optics and Multiphoton Microscopy

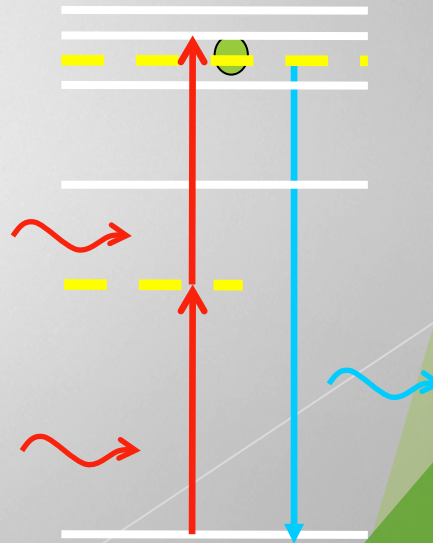
- Minimally invasive
- Deeper penetration
- Reduced photon damage



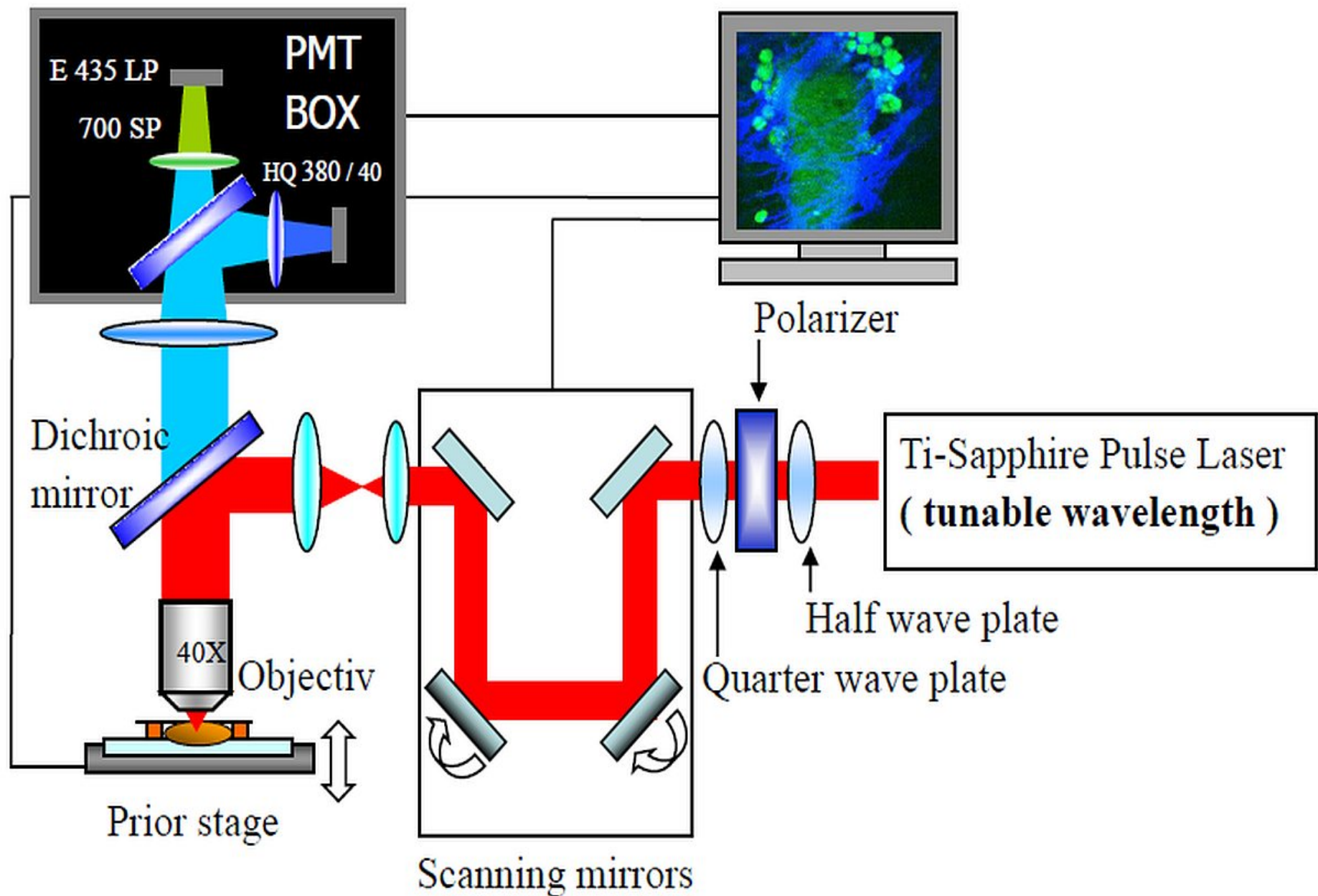
One photon



Two - photon



SHG



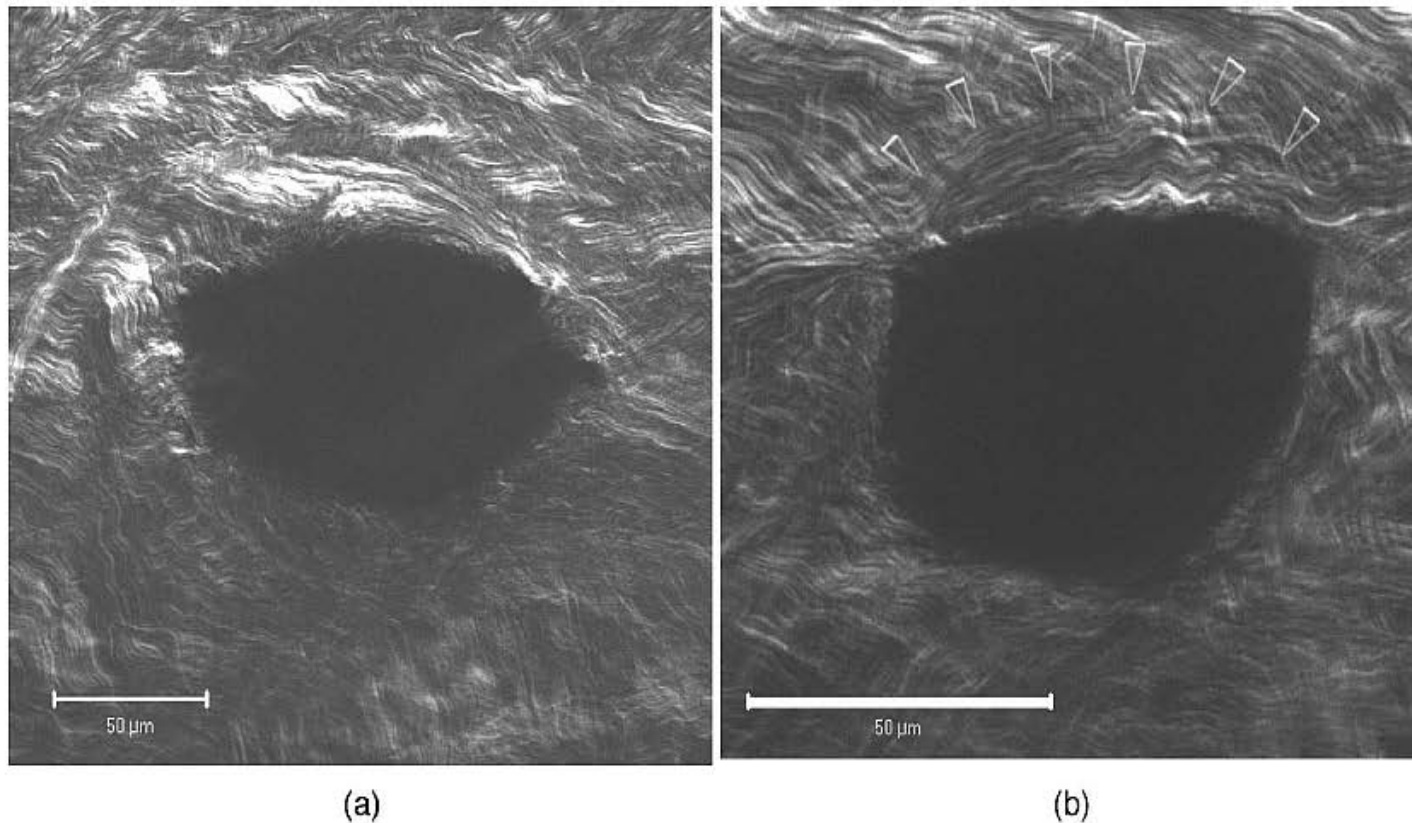
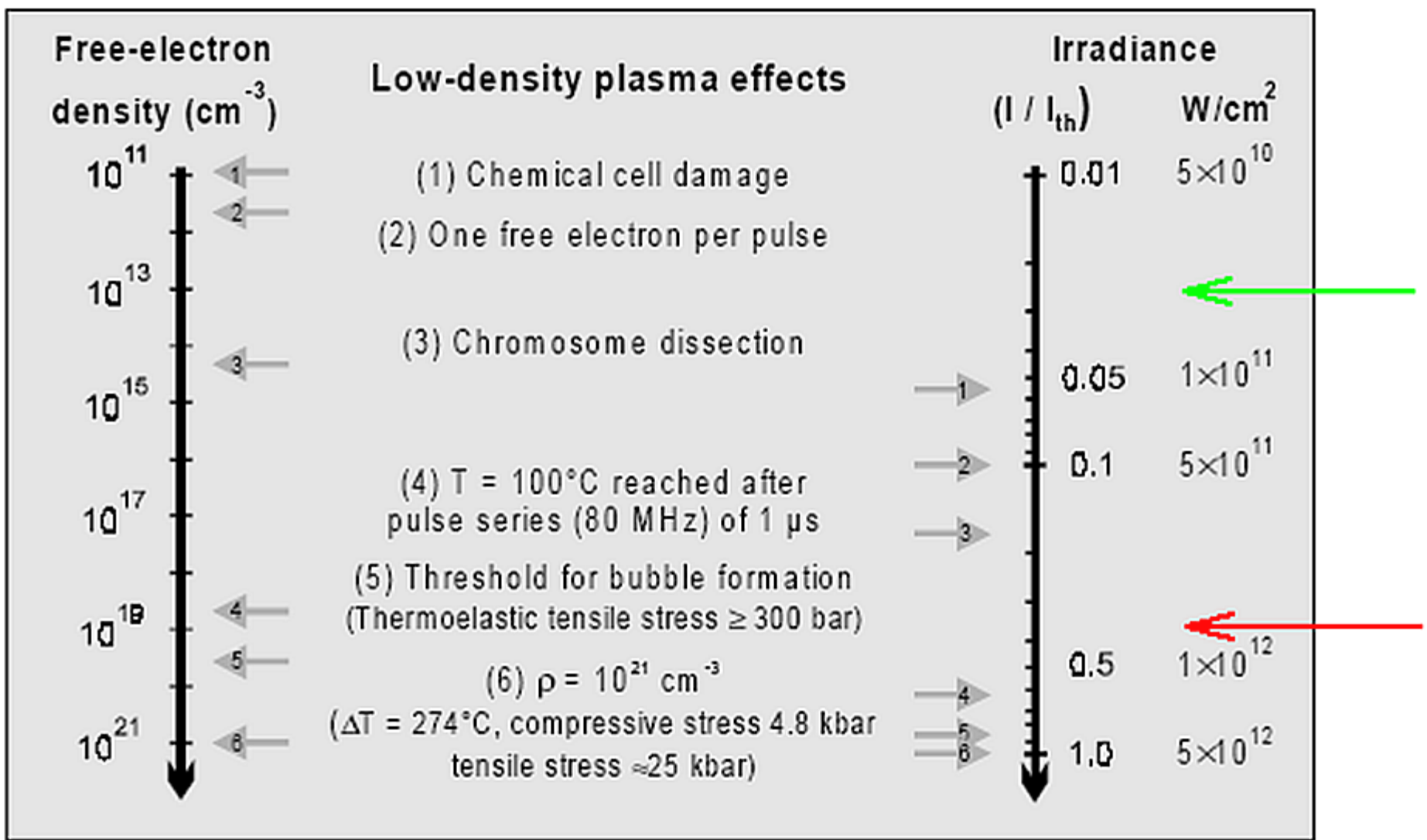


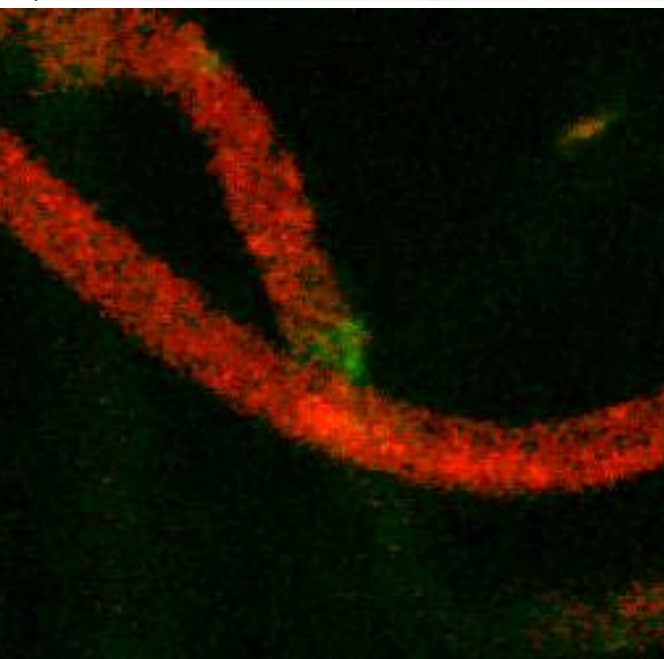
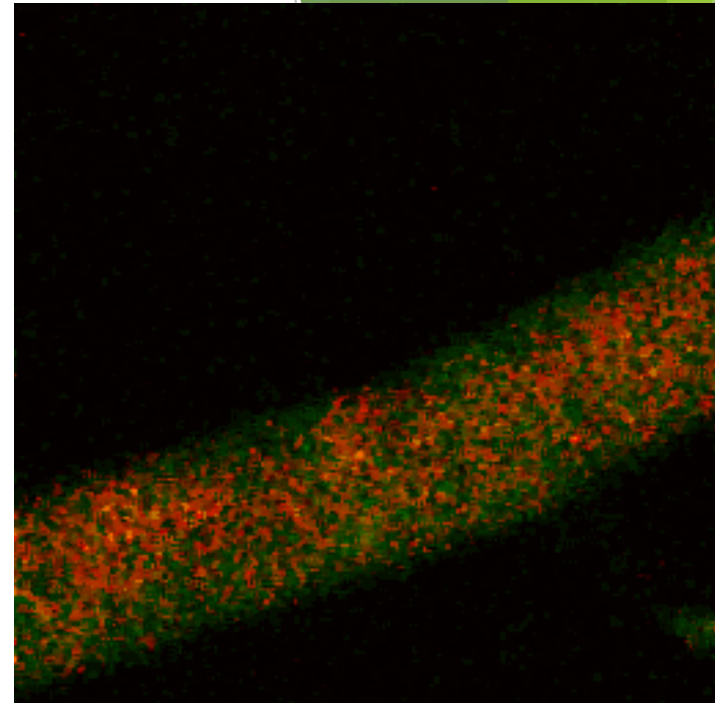
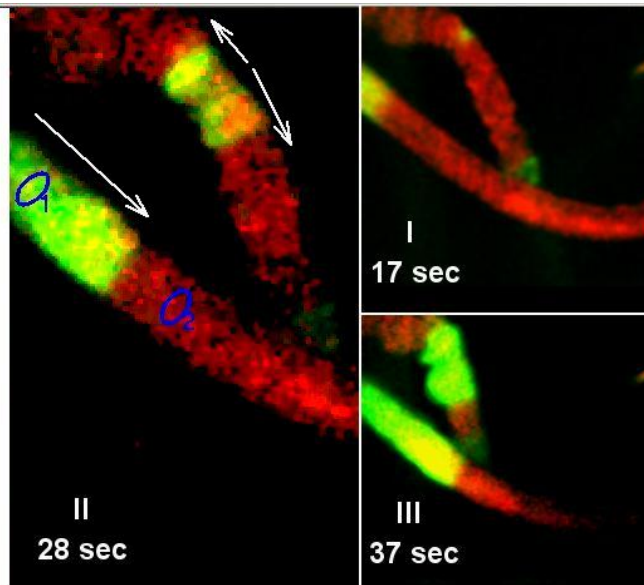
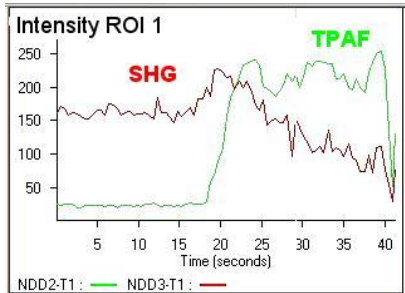
Fig. 4 SHG imaging of two cavitation bubbles each induced by a single-pulse intrastromal fs laser ablation. Bar=50 μm .

“Second-harmonic imaging of cornea after intrastromal femtosecond laser ablation” M.Han, L. Zickler ,G. Giese et al
Journal of Biomedical Optics 9(4), 760–766 2004.



Low-density Plasma effects and breakdown phenomena induced by FS laser pulses. The irradiance values also are normalized to the optical breakdown. Critical electron density of $\rho_{cr} = 10^{21} \text{ cm}^{-3}$

Multiphoton Imaging (MPI) of single rat tale tendon FS laser modification



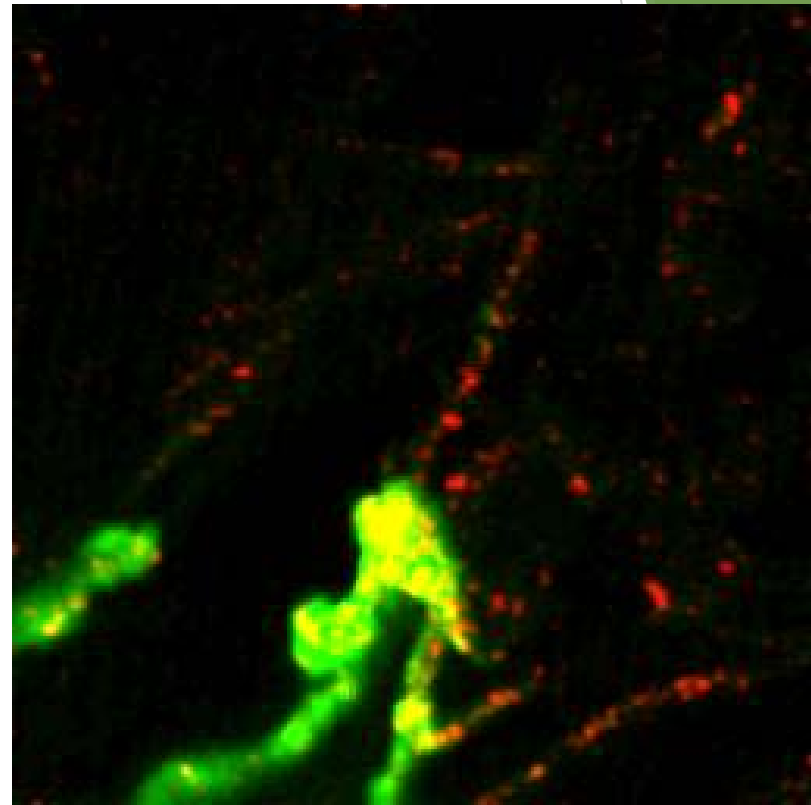
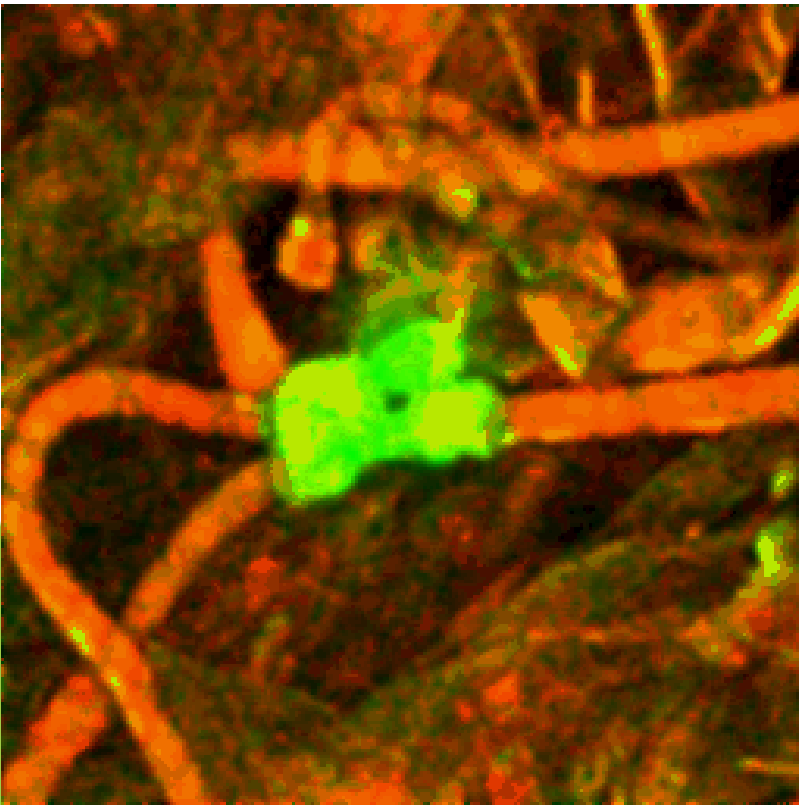
Real time **multiphoton imaging (MPI)** of FS laser photomodification and destruction of single rat tale tendon. **Green pseudo-color-TPF** (435-700 nm) and red **pseudo-color-SHG** (390 nm). Laser power- $P=6$ mW.

Frame size $6 \times 6 \text{mm}^2$.

“Dynamics of femtosecond laser photomodification of collagen fibers,”

V. Hovhannisyan, W. Lo, et al. *Opt. Express* **16**, 7958-7968 (2008).

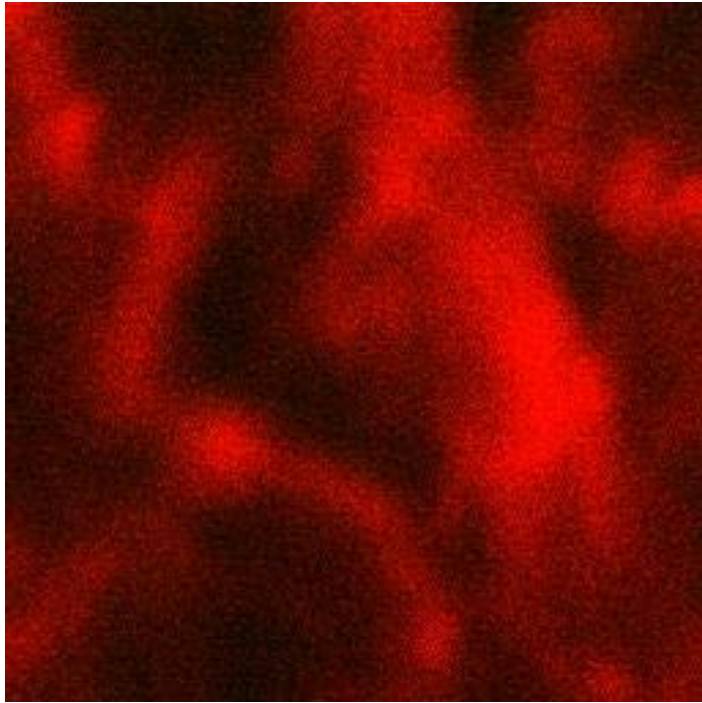
FS laser photodestruction of collagen network from bovine Achilles tendon



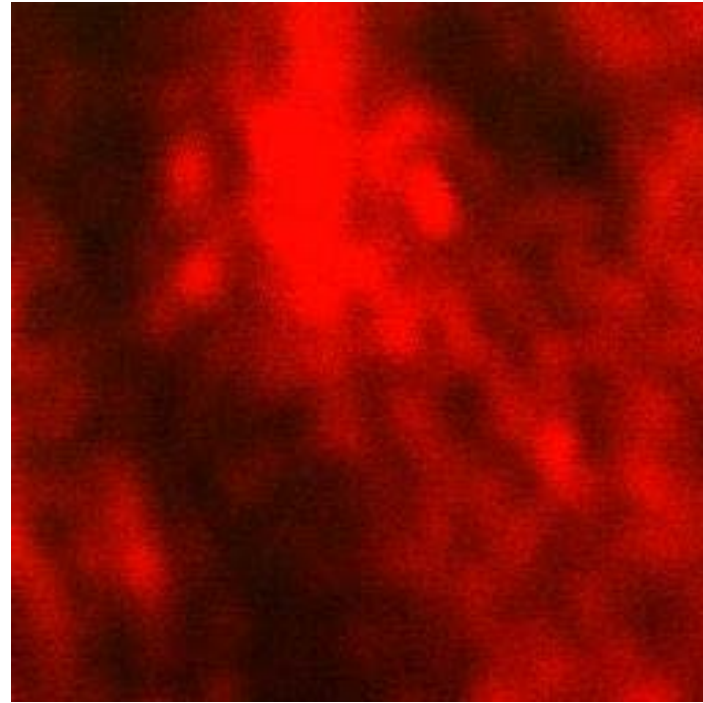
20 μm



FS laser destruction and real time MPI of chicken leg tendon at different laser powers

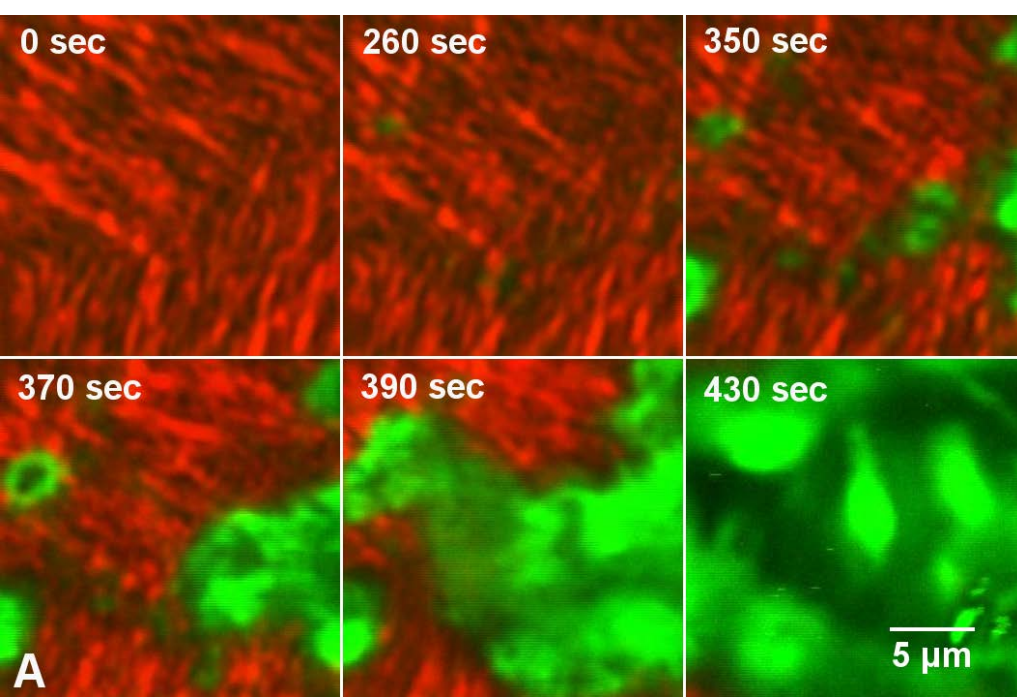


B- P=28 mW

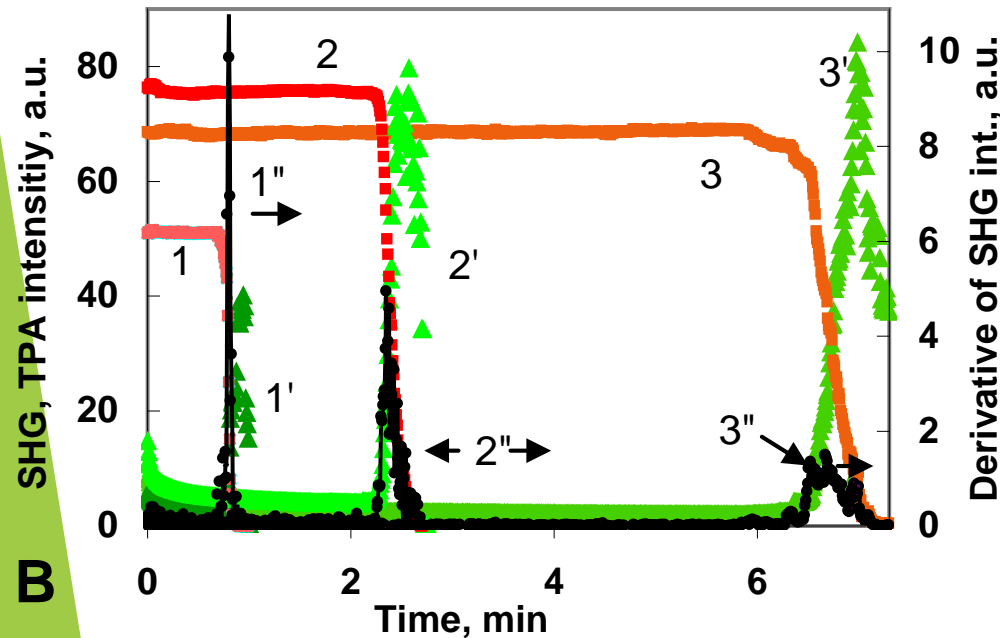


A- P=34 mW

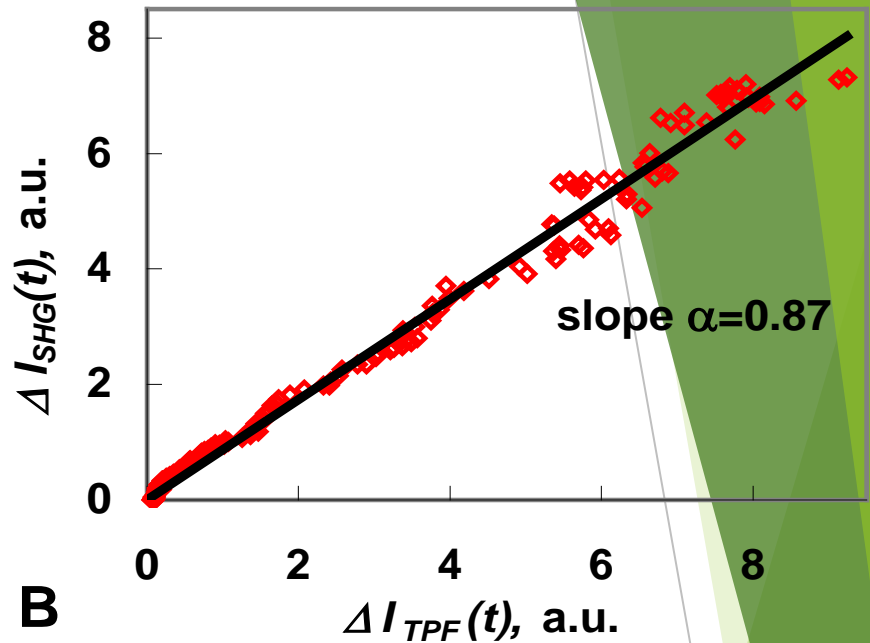
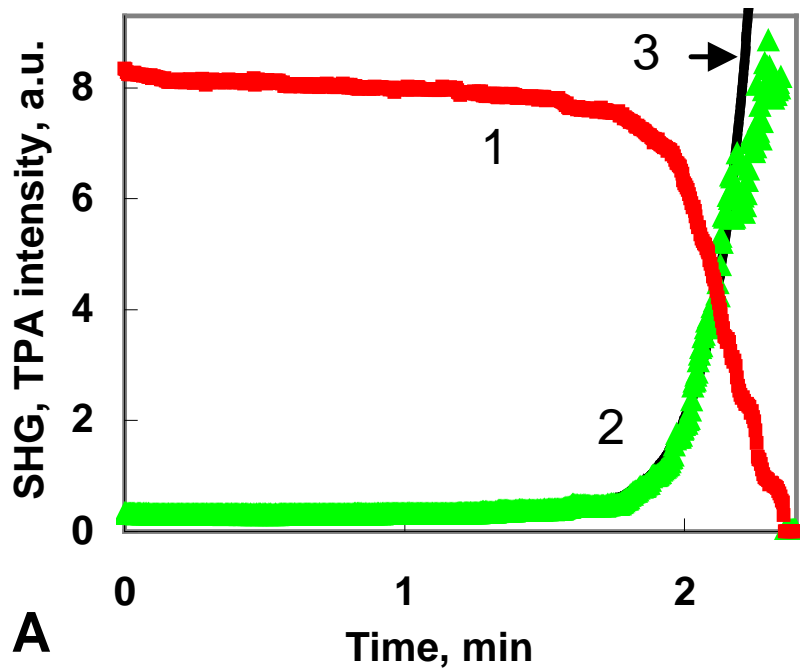
Frame size -12 μm^2 , pixel resident time- 3.2 μs , imaging frequency -2 Hz. Objective- Plan-Neofluar 20x/0.5 NA.



Time-lapsed MPI of dried bovine leg tendon photo-modification at the laser power $P=30$ mW. Red: **SHG**. Green: **TPF**. 20x/NA 0.5 objective was used.



B. Kinetics of SHG (1-3) and TPF (1'-3') signals from **FS** laser illumination at $P=34.5$ mW (1, 1'), 28 mW (2, 2') and 24 mW (3, 3'). 1''-3'' are derivative curves of 1-3 series.



Kinetic analysis of the CFP process in bovine leg tendon A. Plots of SHG intensity $I_{SHG}(t)$ (1), TPA intensity $I_{TPA}(t)$ (2), and exponential fit of $I_{TPA}(t)$ (3) as a function of time. B. Plot of $\Delta I_{SHG}(t) = I_{SHG}(\max) - I_{SHG}(t)$ vs. $\Delta I_{TPF}(t) = I_{TPF}(t) - I_{TPF}(\min)$ for 0-2.5 min period. Objective: 20x/NA 0.5 objective, $P=30$ mW.

$A(t) = \alpha \Delta I_{TPA}(t) = A_0 \exp(Kt)$ and A_0 is the proportionality factor.

$dA/dt = -dC/dt = KA_0 \exp(Kt) = KA(t)$

$$\frac{dC(t)}{dt} = -kC(t)A(t) \quad A(t) = N - C(t)$$

$$C(t) = N / (1 + \exp(Nkt + \ln(A_0 (N - A_0))))$$

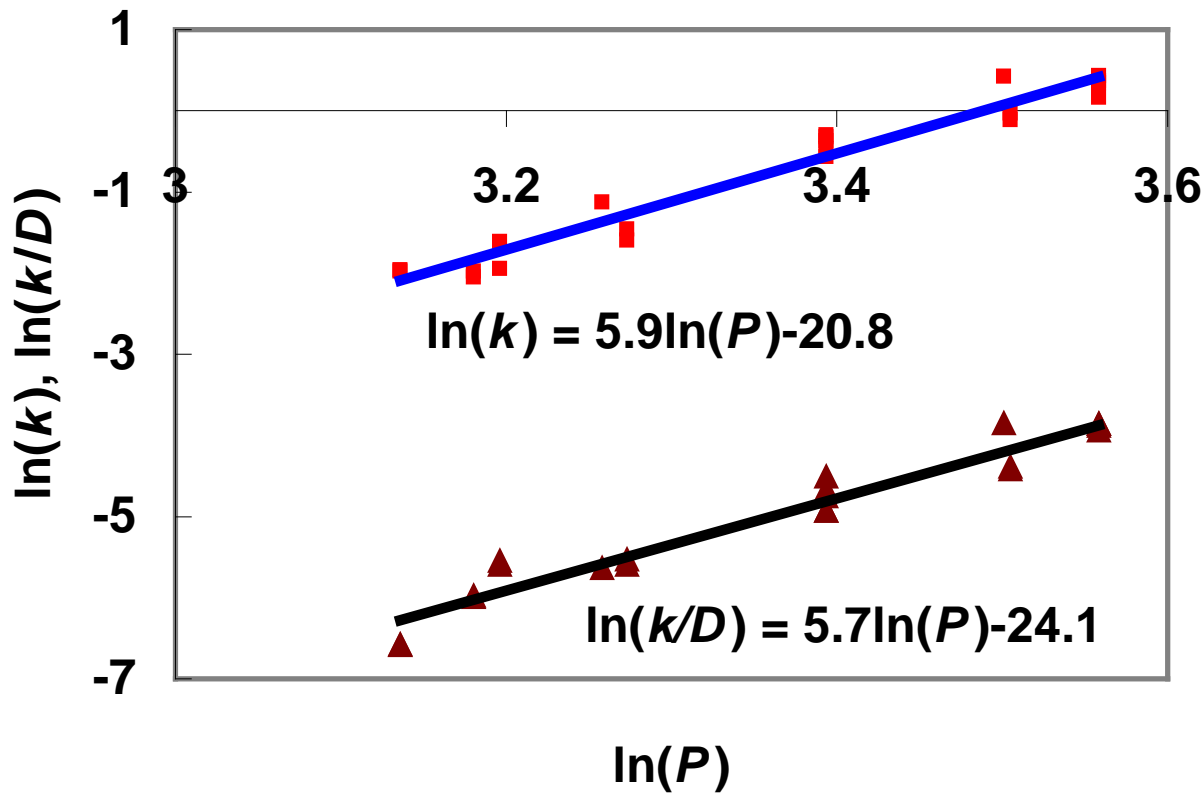
N- initial concentration of native collagen,

$C(t) \sim I_{SHG}(t)$ –current concentration of native collagen;

$A(t) \sim I_{TPF}(t)$ - concentration of collagen photoproduct;

k- photomodification rate, which strongly depends on irradiation laser intensity;

$A_{(0)}$ is initial small concentration of photoproducts at $t=0$,

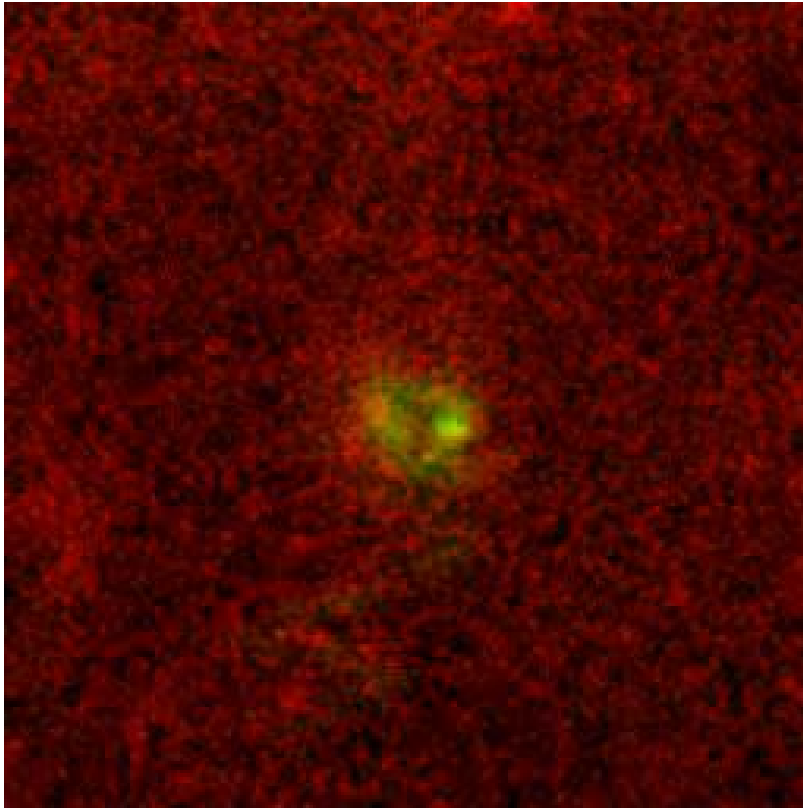


Dependences of $\ln(k)$ and $\ln(k/D)$ on $\ln P$ for bovine leg dry tendon.

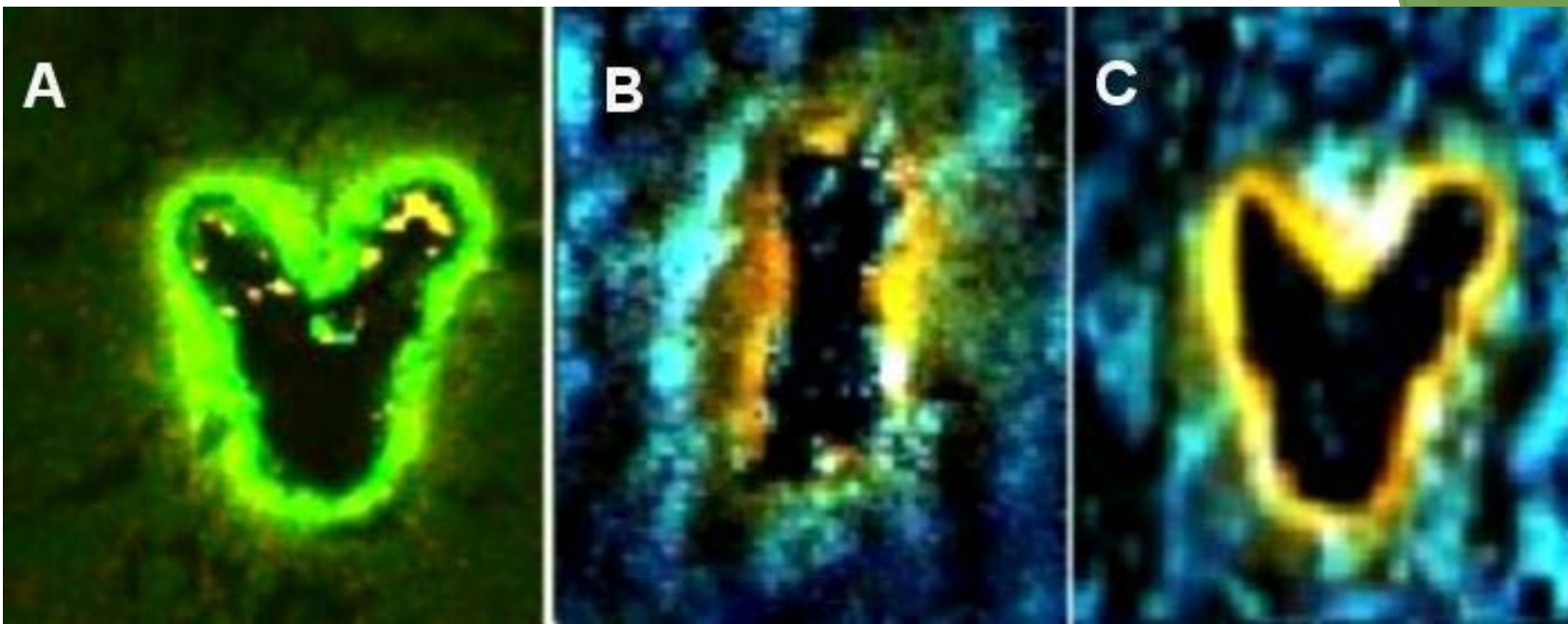
Here we set N as 1 and $\ln(A_0/(N-A_0))$ as D .

The slopes for $\ln(k)$ is 5.9 ± 0.3 and for $\ln(k/D)$ 5.7 ± 0.3

Collagen fiber destruction in bovine cornea

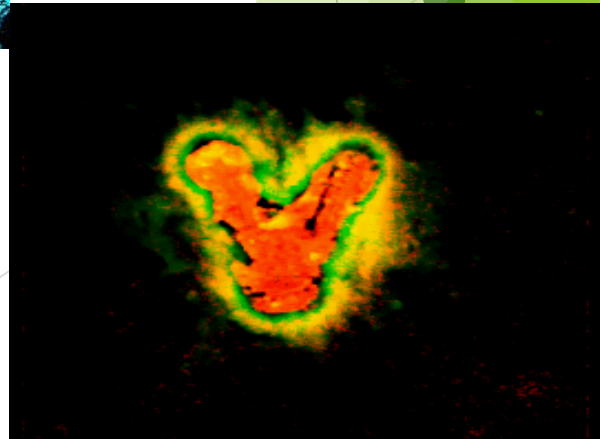
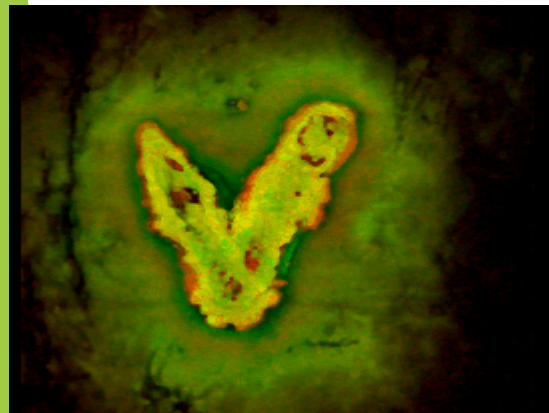
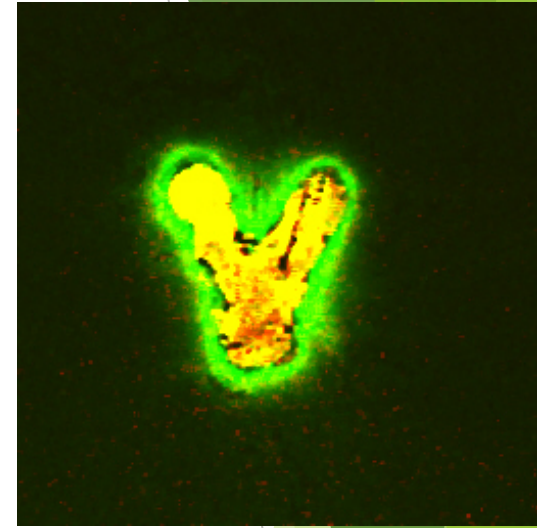
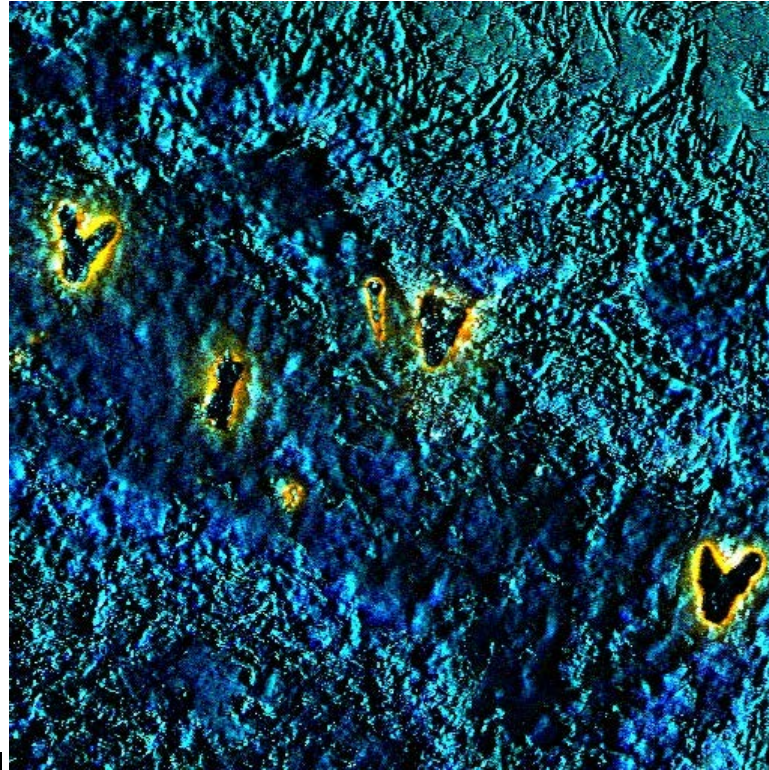
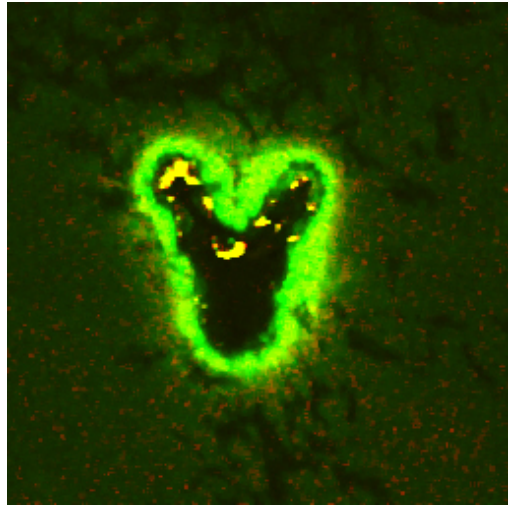


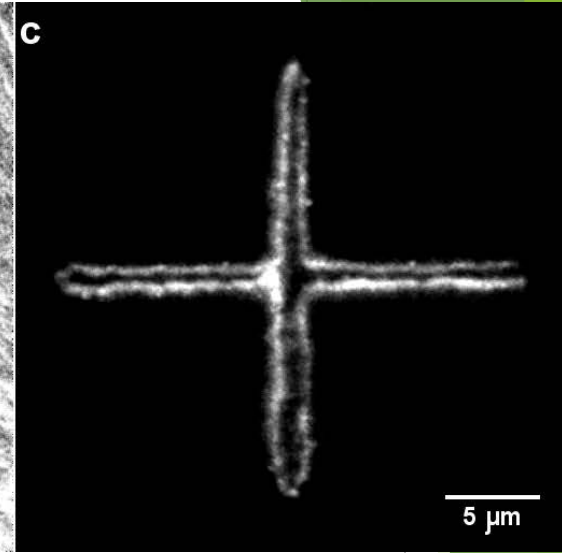
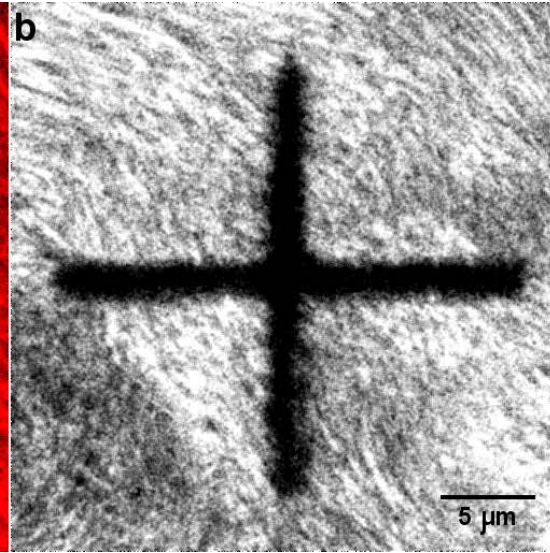
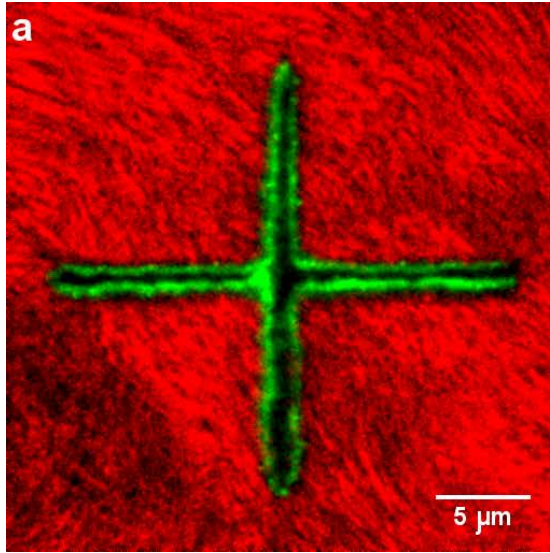
$P=21\text{mW}$, frame size $11.5\ \mu\text{m}$



FS laser lithography in bovine corneal stroma. The letters “V” ((A) and (C)) and “I” (B) were sculptured with 20 mW of FS laser. Image (A) was acquired using FS laser with power of 5 mW (red: SHG; green: TPAF). (B) and (C) are confocal images (blue: reflected confocal signal at 458 nm; green: autofluorescence between 505-550 nm; red: autofluorescence between 550-670 nm). (Frame height: 17 μ m).

Collagen fiber destruction and FS laser manipulation in bovine cornea



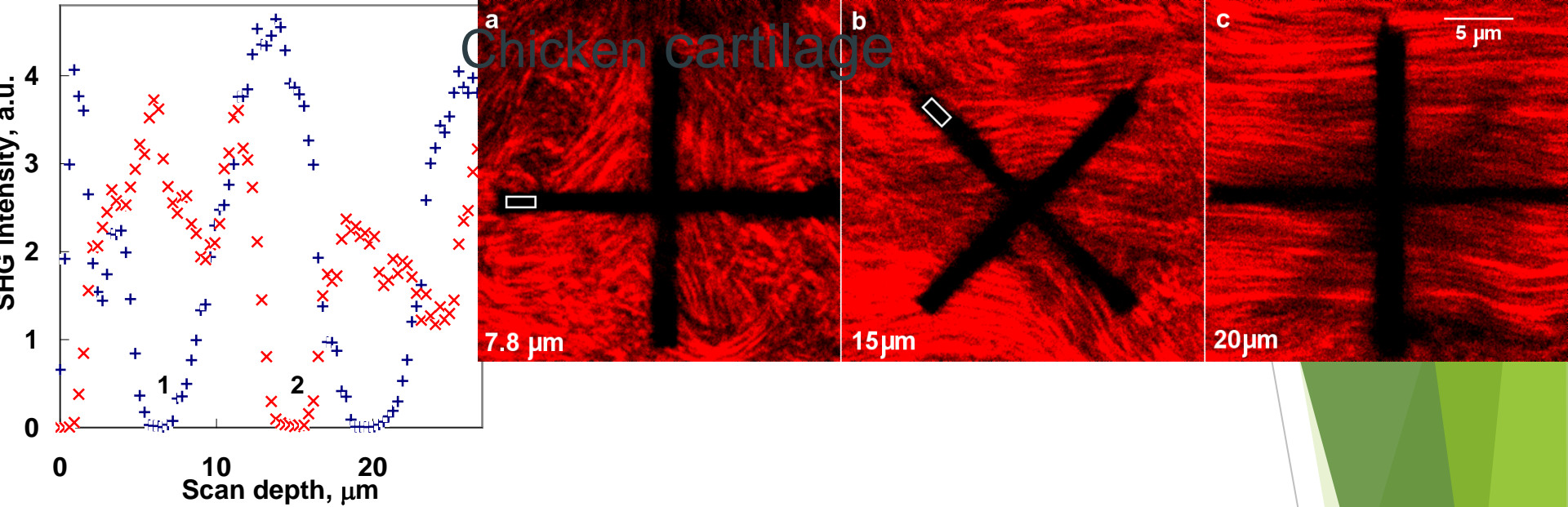


A crossed pattern was engraved at the depth of 160 μm in chicken leg bone cartilage tissue by the scanning of two perpendicular rectangles $1 \times 23 \mu\text{m}^2$ in size using 40 sec of focused illumination at $P=30$ mW. The objective: Fluar 40x/NA 1.3_oil.

a. Combined SHG (red) and TPA) (green) image.

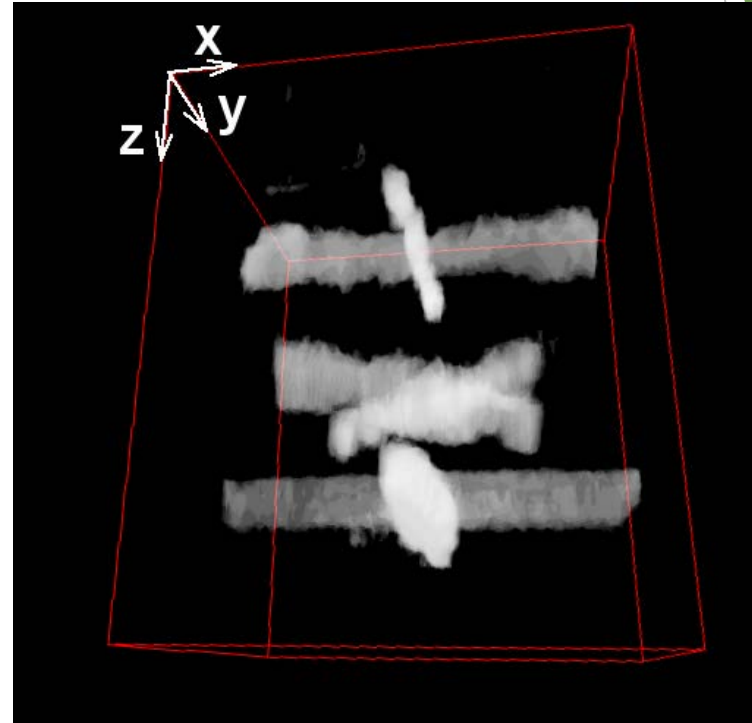
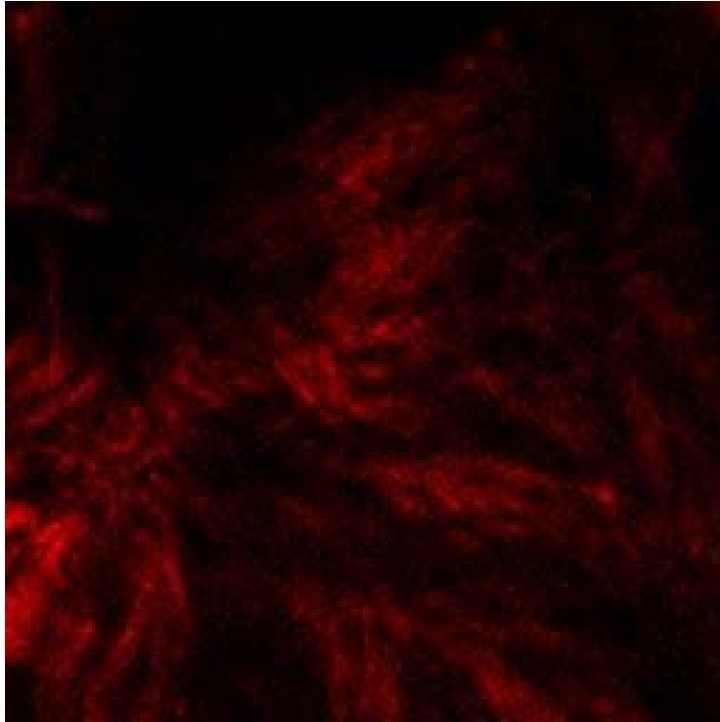
b. SHG image illustrates photomodification of collagen fibers inside the illuminated area.

c. TPA image illustrates the formation of photoproducts.



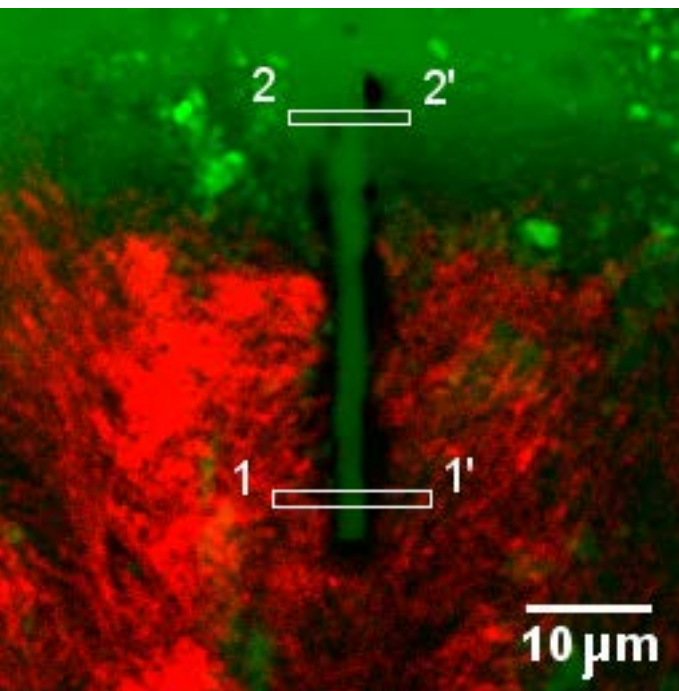
3D engraving of cross patterns in chicken leg bone cartilage matrix by FS laser using the Fluar 40x/NA 1.3 oil objective. Two cross patterns were engraved at the depths of $7.8 \mu\text{m}$ ($P=20 \text{ mW}$) and $20 \mu\text{m}$ ($P=60 \text{ mW}$), and the third cross pattern oriented at 45° relative to the first 2 patterns, was engraved at the depth of $15 \mu\text{m}$ ($P=40 \text{ mW}$). Axial profiles of SHG intensity in two regions are shown. Profile 1 passed through the two engraved patterns “+” and the profile 2 passed through the engraved sign “x”.

3D SHG image of the photomodified chicken leg bone cartilage

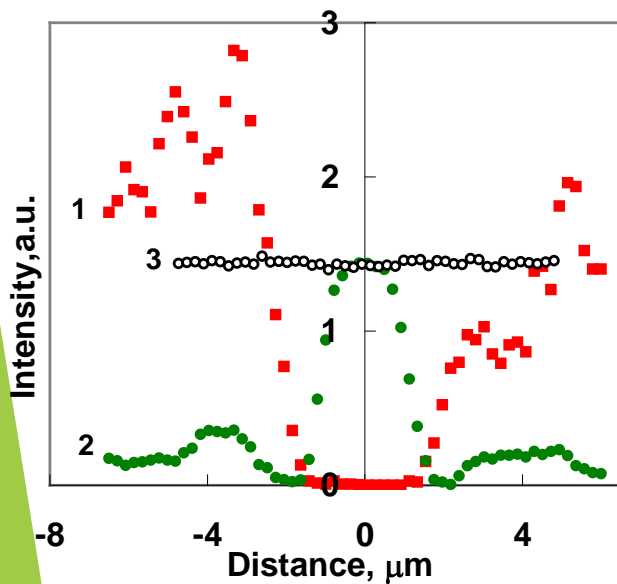


3D MPI of the photomodified tissue. Scan volume $26 \times 26 \times 27 \text{ mm}^3$, and optical sections were acquired at the intervals of $0.3 \text{ }\mu\text{m}$. B.

White color indicates the photomodified sites.

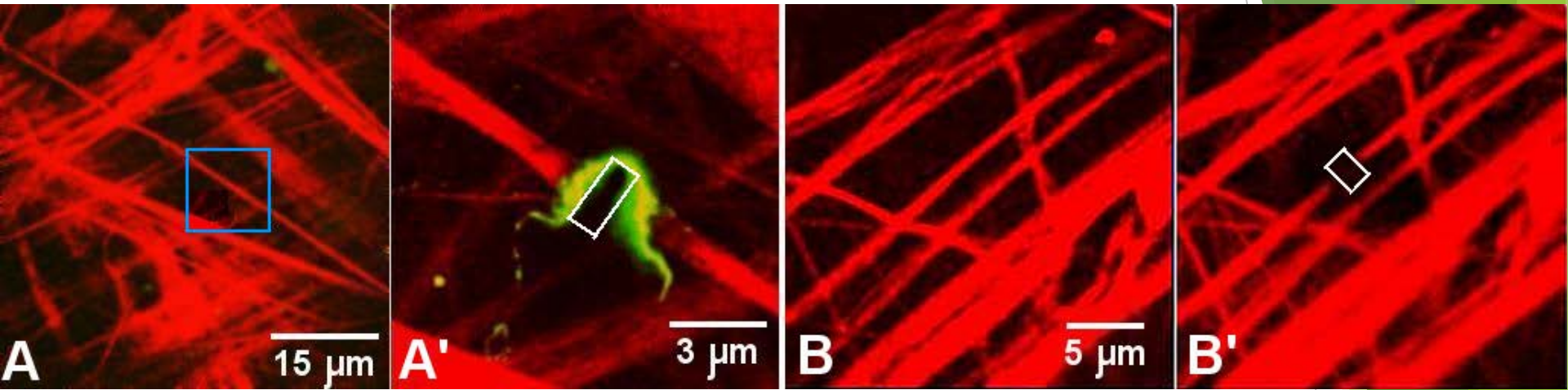


A. MPI of cartilage tissue dipped in rhodamine B (RB) solution after $P=30$ mW of 1 min illumination in creating a rectangular ($1 \times 40 \mu\text{m}^2$) pattern. RB solution flowed into the cavity engraved by fs laser at the depth of 3 mm. Green is TPF of RB and red is collagen SHG signals.



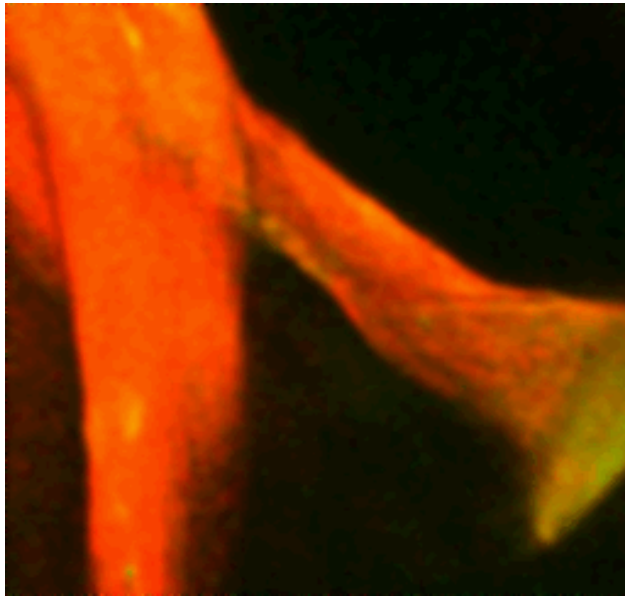
B. Intensity profiles of TPF (1) and SHG (2) along the 1-1', and TPF (3) along the 2- 2' bars

FS-laser cutting of single collagen fibers deep in chicken skin

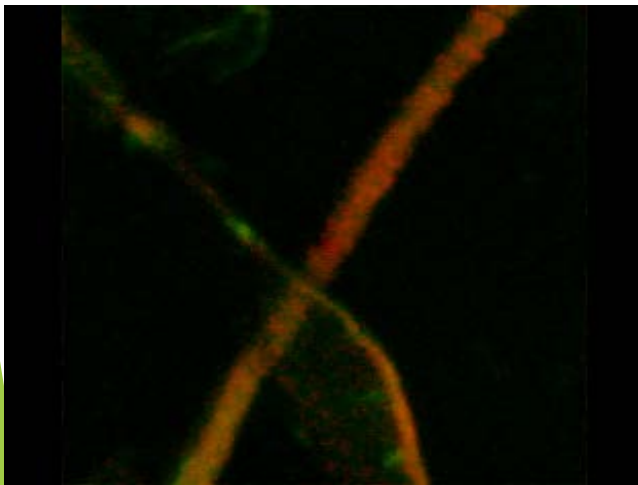
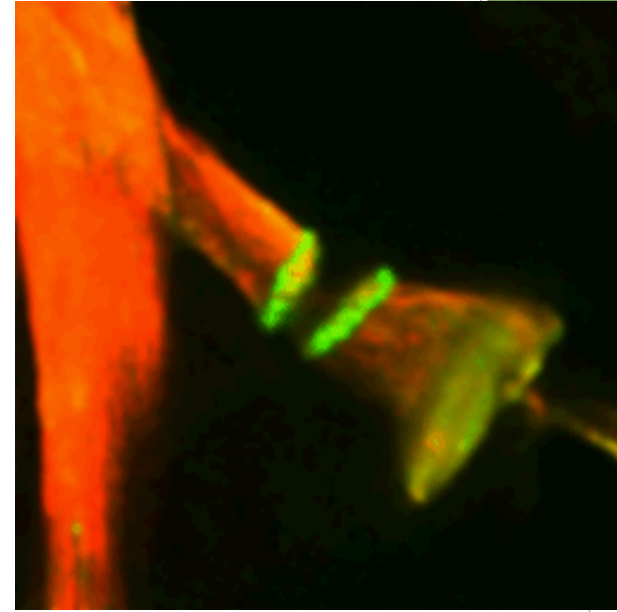


MPI of two sites in wet chicken skin dermis before (A, B) and after (A', B') 50 mW FS laser illumination of the selected regions of interest. A' is an image of the blue squared region marked in A after 20 sec of fs laser illumination. B' is the image of B after 30 sec illumination. TPF of the generated photoproduct that was seen after the short time illumination (A'), vanished after longer fs laser illumination (B').

Collagen FS laser cutting (A) and welding (B)

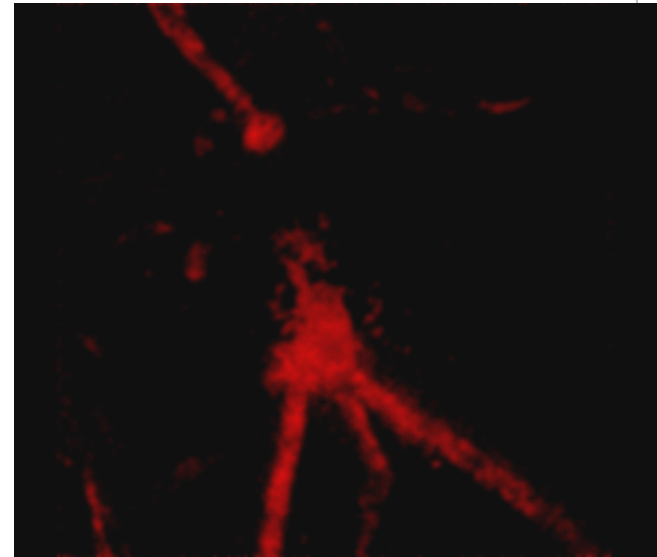


A



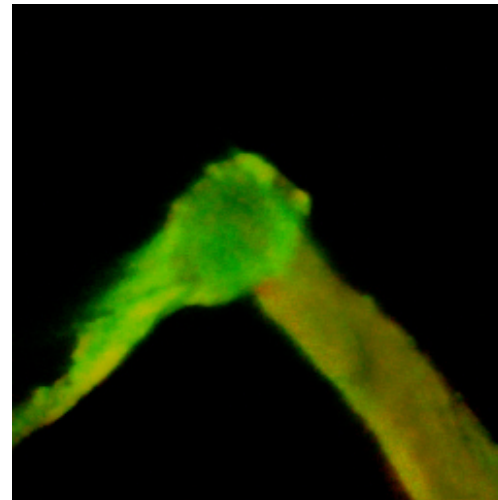
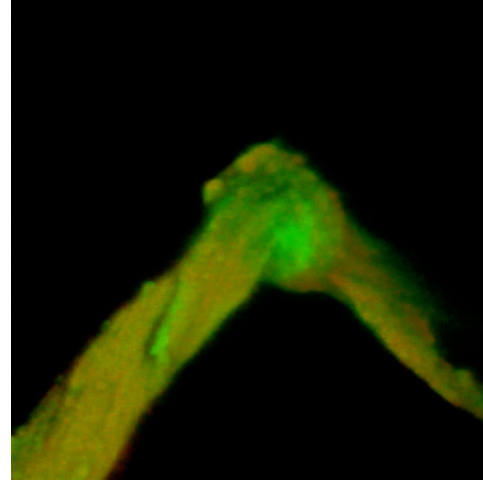
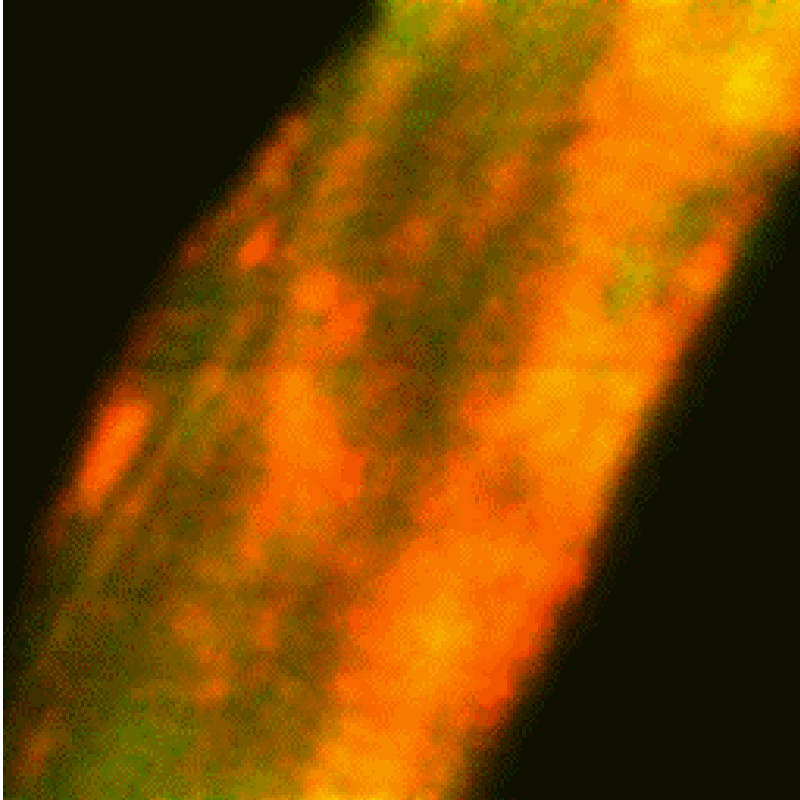
Before irradiation

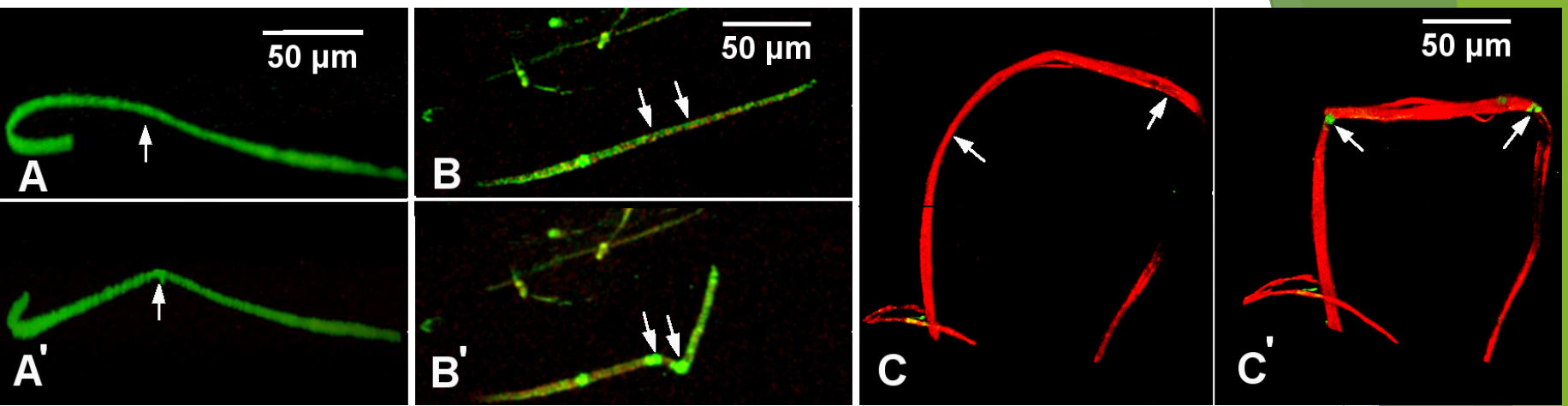
B



After irradiation

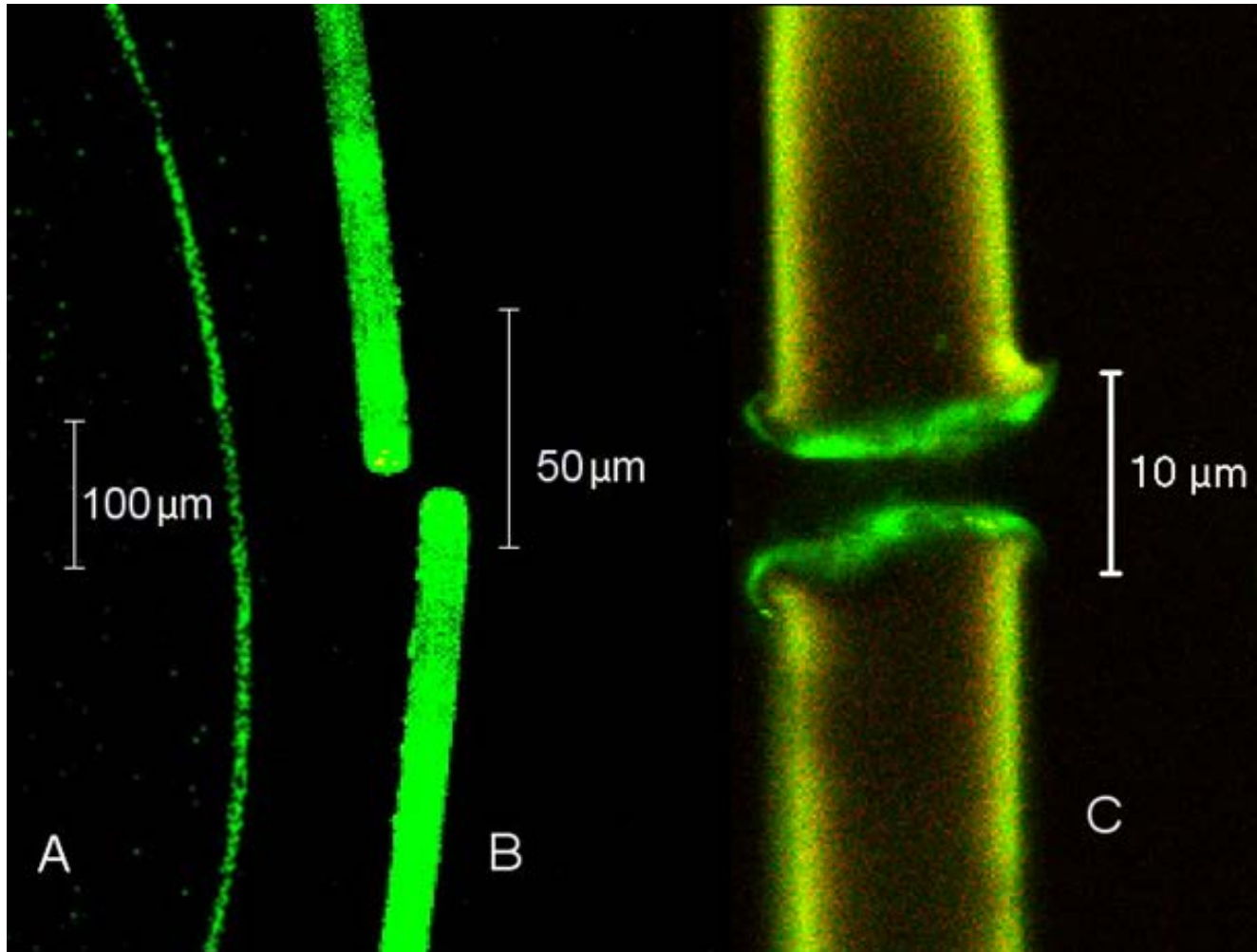
Collagen fiber FS laser bending

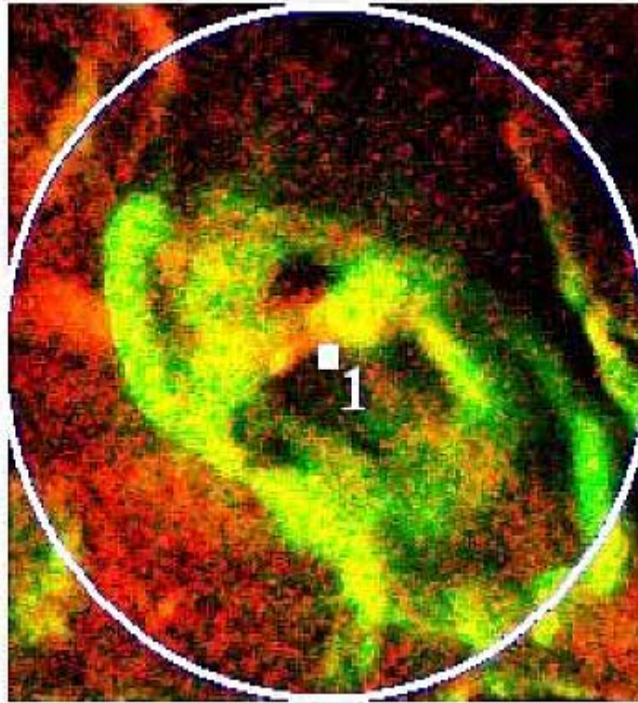
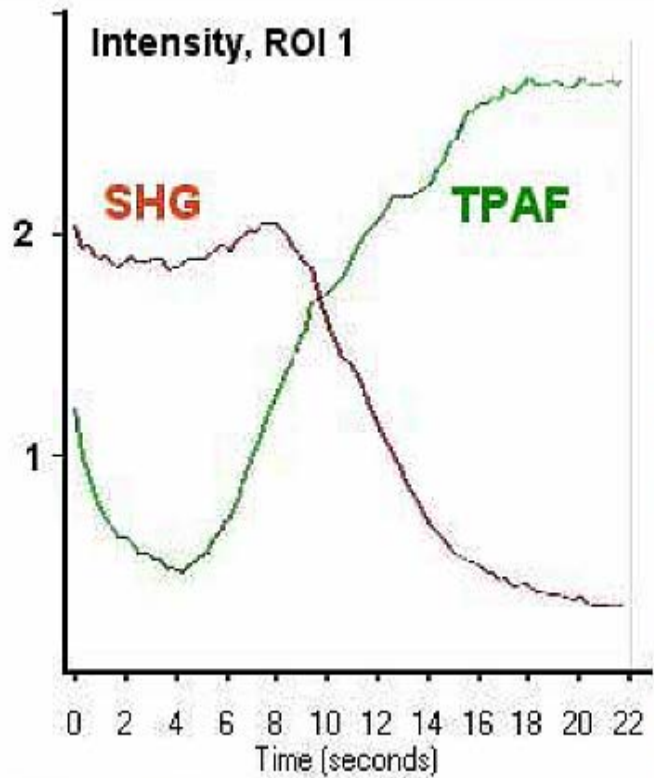




Bending of collagen fibers from FS laser illumination of dry RTT (A, A'), BAT (B, B'), and chicken leg tendon (C, C'). A, B, and C - collagen fibers before photomodification and A', B' and C' are the images after FS modification. Laser powers were 20 (A and B) and 40 mW (C). The photomodification regions (one site in A and two sites in B and C) are indicated by arrows.

FS laser cutting of silk (A,B) and polymer (C) fibers





Time dependence of TPF(green) and SHG(red) intensities during the FS laser scan within a collagen fiber network from bovine Achilles' tendon. The laser power was 29 mW. Frame size 46x46 μm^2

“Dynamics of femtosecond laser photo-modification of collagen fibers” V. Hovhannisyanyan, W. Lo, C. Hu, S.J. Chen, C.Y. Dong
Optics express 6(11)7958-68, 2008.

1st option- the use of **high power** laser formation of **micron-sized gas bubbles** in the corneal stroma.

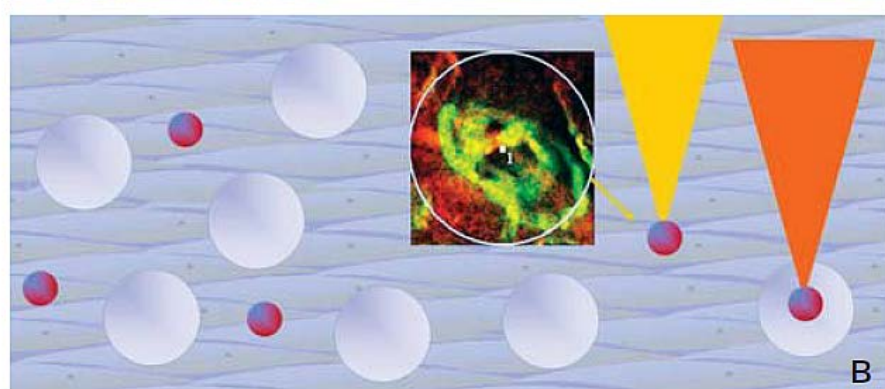
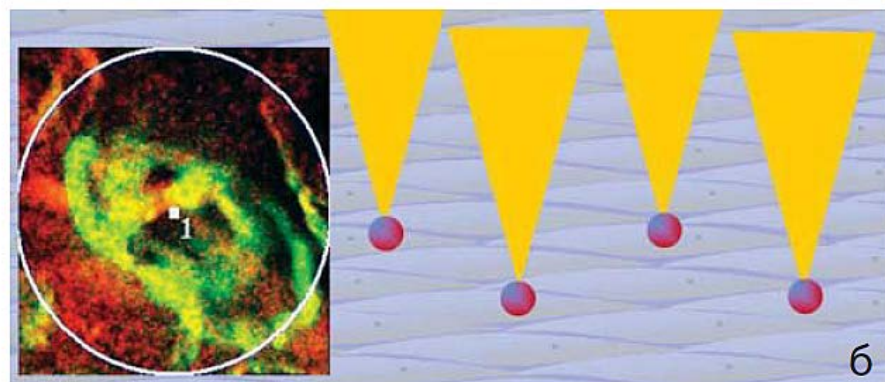
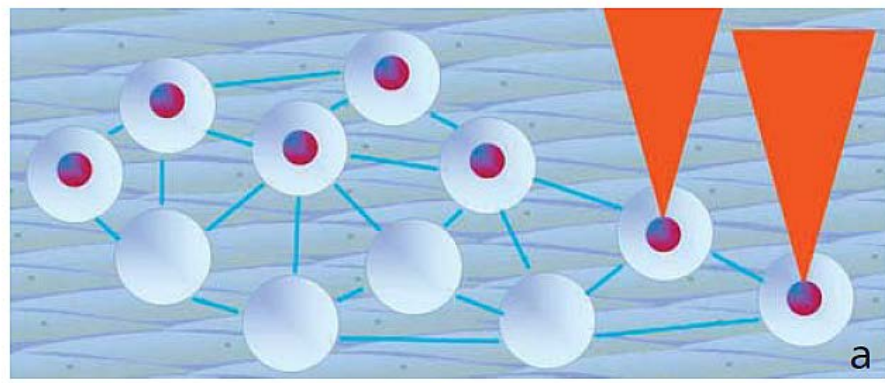
2nd option- the use of **low radiation** sufficient to effect **photochemical interaction**, but below the **threshold of plasma bubble** formation.

3th option - combination of the **micro-ablation** and **photochemical modification**.

Novel non-invasive technologies for laser modification of ocular optic refractive structures

I. M. Kornilovskiy,
National Medical Surgical Center, Moscow, Russia

Refractive surgery and ophthalmology
Vol. 9, No. 3 17-26. 2009.

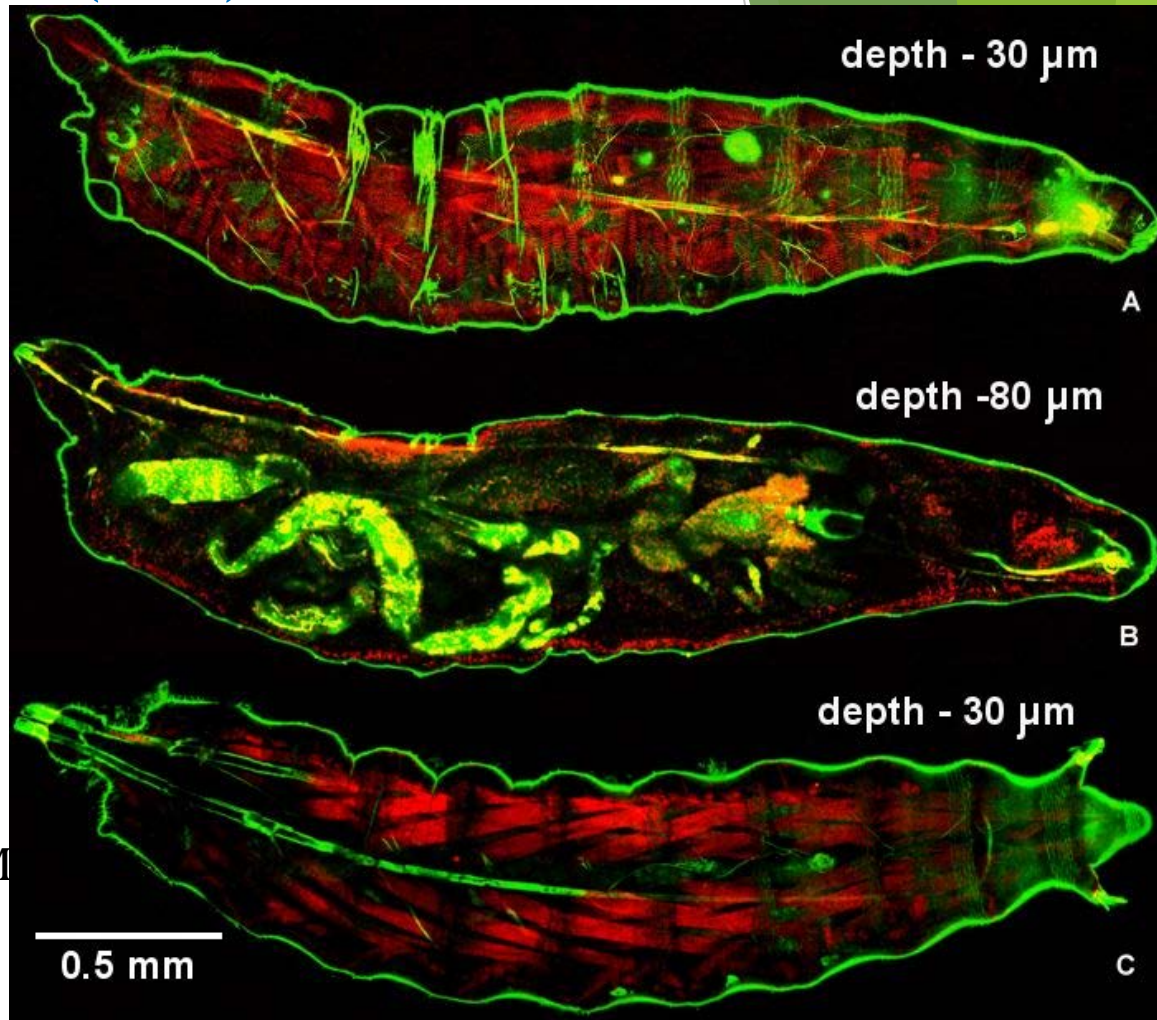


Drosophila melanogaster (DM) model for MPI

Drosophila melanogaster: 75% of human disease-causing genes have a functional homolog in DM.
DM in biomedical research:

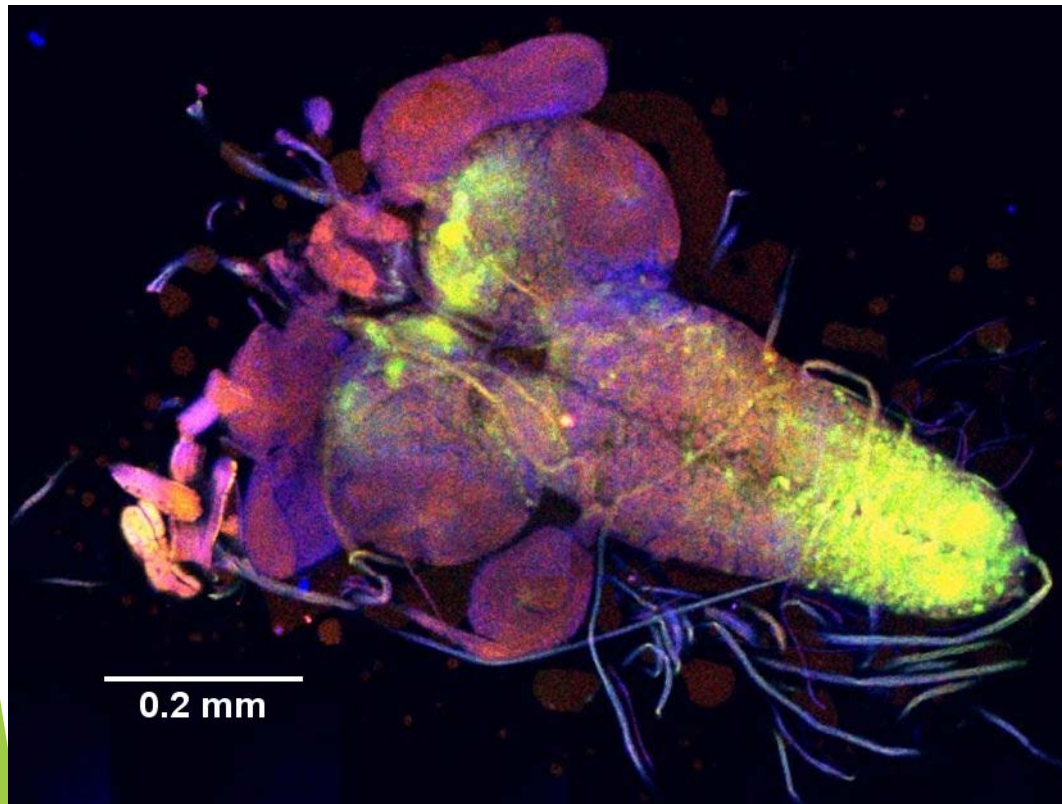
- Central nervous system disease,
- Cardiovascular disease, Cancer,
- Diabetes,
- Drug development/screening and target discovery.

Side views (A and B) and top view (C) of the second stage DM larva. Whole-body, depth-resolved TPF (green) and SHG (red) images of DM were acquired *in vivo* using multiphoton microscope based LSM510 system and ti:sa femtosecond laser, $\lambda_{exc} = 780$ nm. Objective-40 \times /NA 1.2.



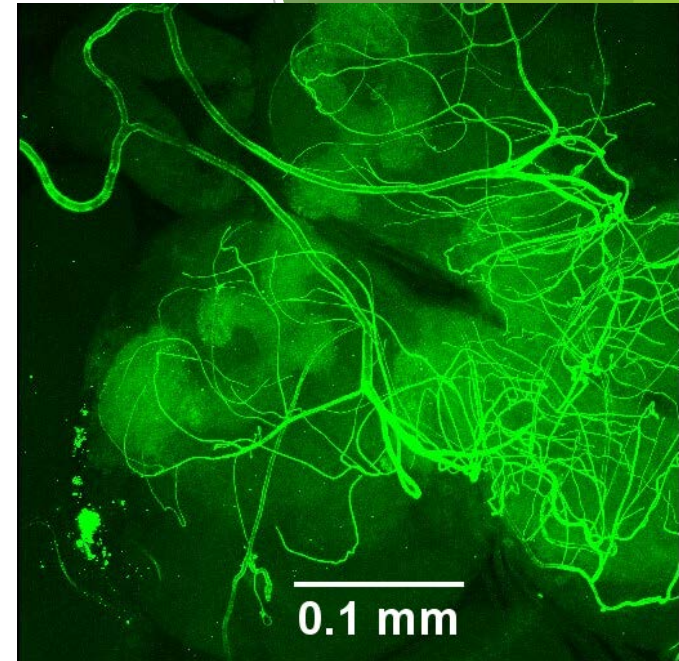
Label-free imaging of Drosophila larva by multiphoton autofluorescence and second harmonic generation microscopy. C. Y. Lin, V. Hovhannisyann, J. T. Wu, et al *J. Biomed. Opt.*, **13**(5), 054003 (2008).

Confocal and multiphoton imaging of DM brain

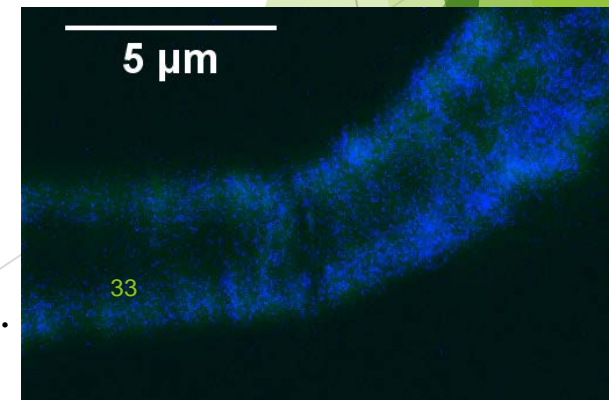


Confocal microscopy of brain of GFP transfected DM.

$\lambda_{exc} = 458$ nm. C-Apochromat
40x/1.2W



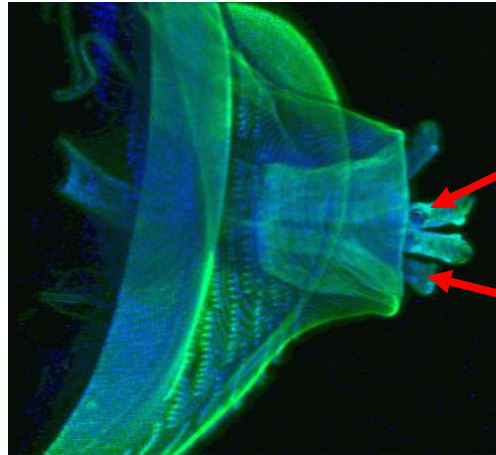
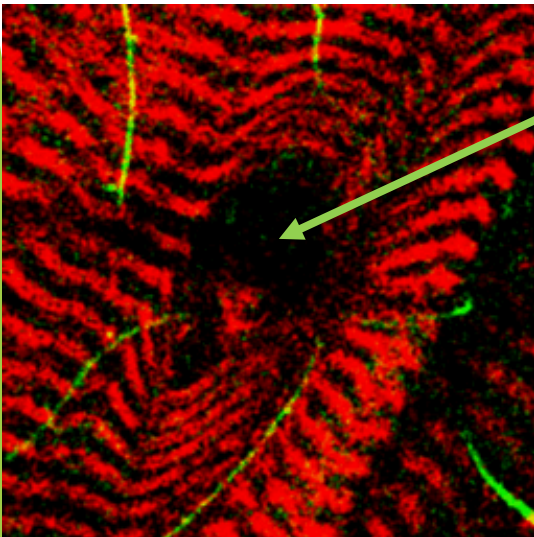
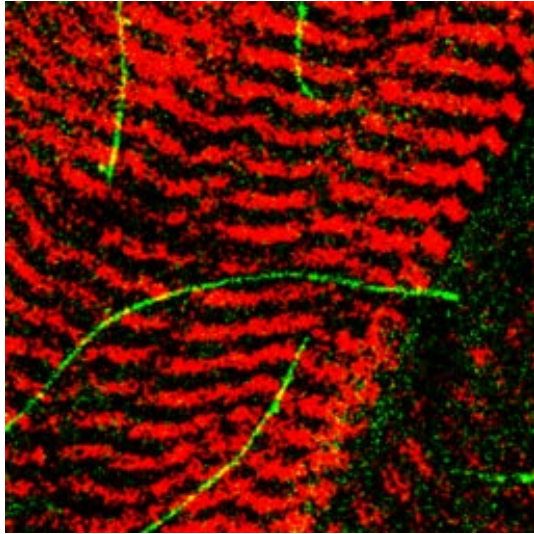
Projection of **3D TPF** image of vascular system providing circulation of hemolymph in DM brain.



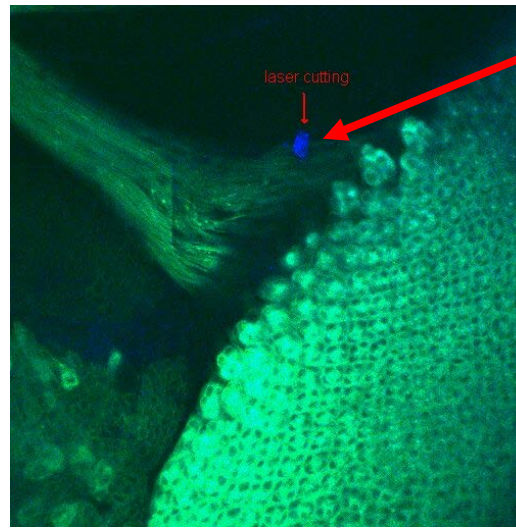
SHG image of DM brain vessel.

FS laser micro-surgery of *Drosophila melanogaster* (DM) organs

Laser ablation of DM nerve-muscle junction



Laser ablation of anterior spiracles



Laser ablation of eye fiber

Frame size $40 \times 40 \mu\text{m}^2$,
 $\lambda_{\text{exc}} = 780 \text{ nm}$.
Objective-40 \times /NA 1.2

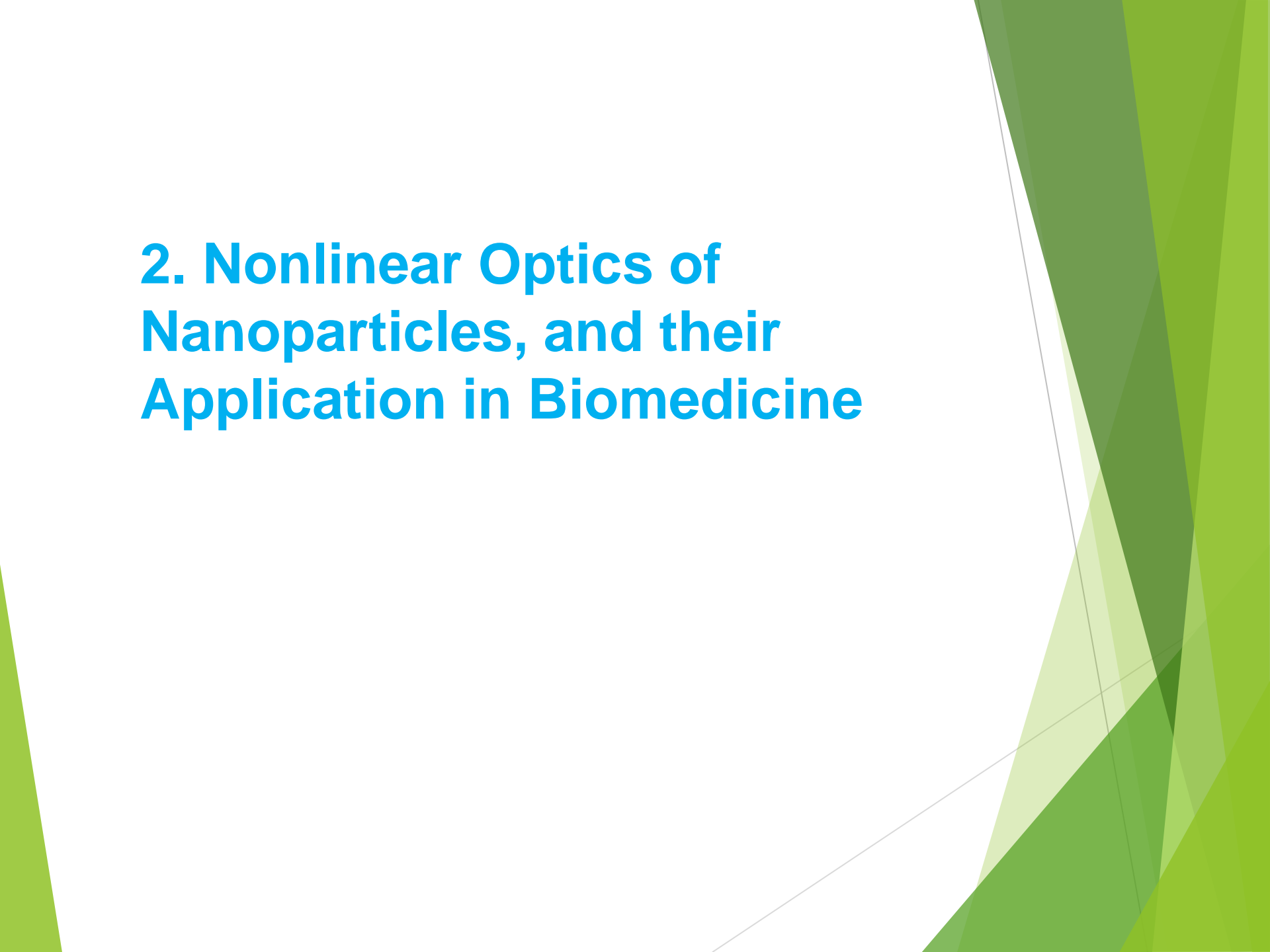
Summary

Non-ablative, mini-invasive, high-resolution laser controlled modification of biological tissue and imaging by FS laser were demonstrated. The micro-modification mediates by free-electron-induced chemical bond breaking and low-density plasma formation followed by chemical effects, and not related to heating or thermoelastic stresses. Using SHG and TPF microscopy it was shown that efficiency of the process depended on the ~ 6 power of the laser intensity. Furthermore, it was demonstrated that the method can be used for bending and cutting of collagen, elastin and myosin fibers and creating 3D patterns within biological tissue with high precision ($\sim 2 \mu\text{m}$).

Application of nonlinear photonic technologies in biomedicine

1. **Tissue engineering and regenerative medicine:** laser microprocessing, cutting, welding and form construction.
2. **Cosmetics:** skin resurfacing, burn- and freeze-produced wounds healing.
3. **Ophthalmology:** Laser-induced trans-scleral ocular hyperthermia, refractive and cornea surgery, noninvasive FS laser treatment of cataract.
4. **Oncology:** Laser surgery and coagulation, TPF monitoring of delivery and accumulation of photosensitizer, fluorescence diagnosis and photodynamic therapy of cancer;
5. **Biomedical Instrumentation:** diagnostics and measuring systems based on nonlinear optics.

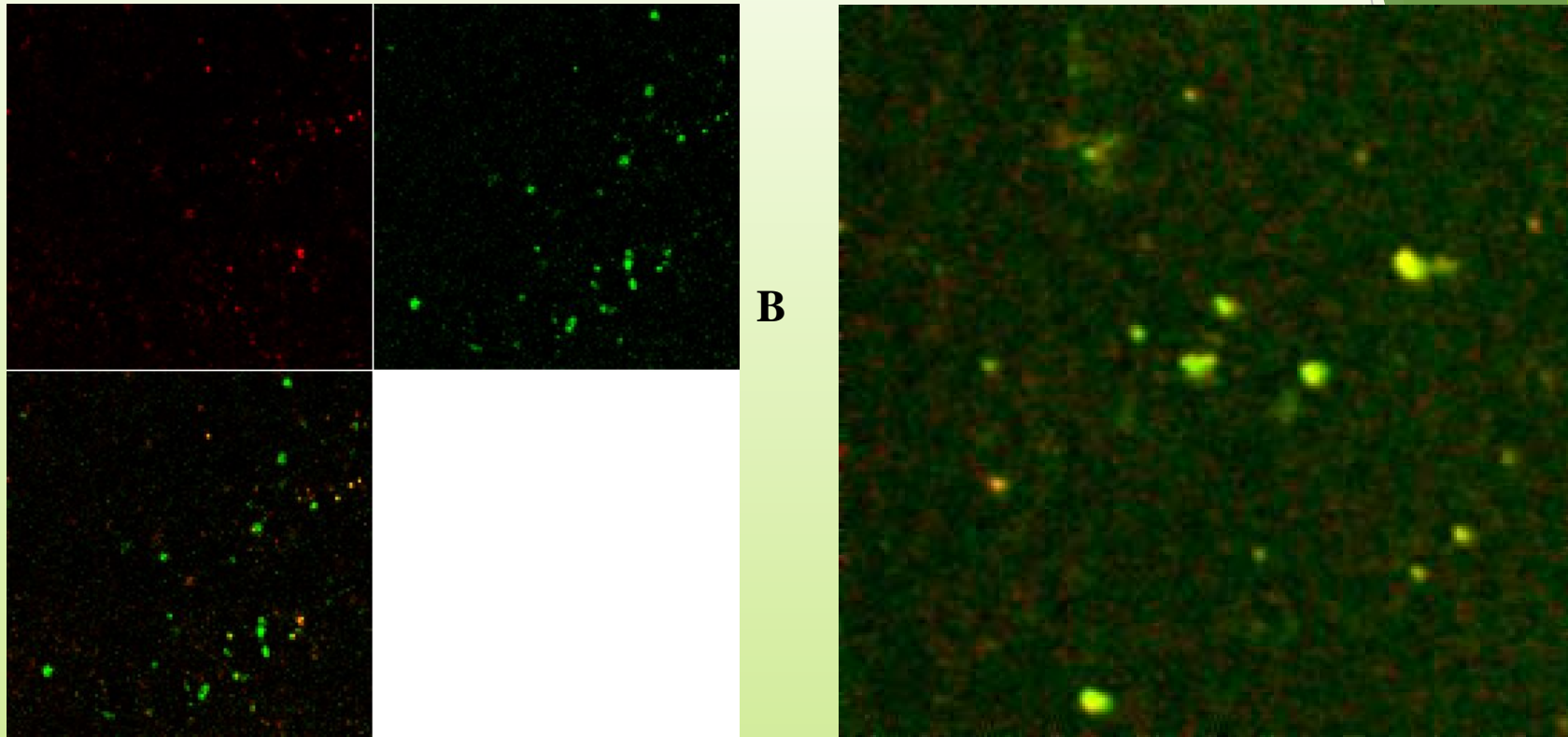
2. Nonlinear Optics of Nanoparticles, and their Application in Biomedicine



Introduction

- **Nanoparticles (NPs)** have been introduced in biomedicine as effective agents for cancer-targeted drug delivery and thermotherapy.
- **Gold (Au)** and **silver (Ag)** based **NPs** have additional advantages because of **Surface Plasmon Resonance Enhancement**, which can intensify electrical, optical, thermal, and chemical processes in local area around **NPs**. The enhancement of the optical response is especially large in case of **multi-photon** induced processes, including **second SHG** and **TPF**.
- We study nonlinear optical properties of **Au**, and **Ag NPs**, and apply these materials in **multiphoton imaging (MPI)** and laser phototreatment of biological systems.
- Using **MPI and nonlinear spectroscopies**, the biodistribution, pharmacokinetics, surface-enhanced phototoxicity and laser induced thermal effect of **NPs** in **cells** and **Drosophila melanogaster (DM)** model will be investigated.
- The research may help to introduce these **NPs** and nonlinear optical approaches into biomedicine and clinical environment.

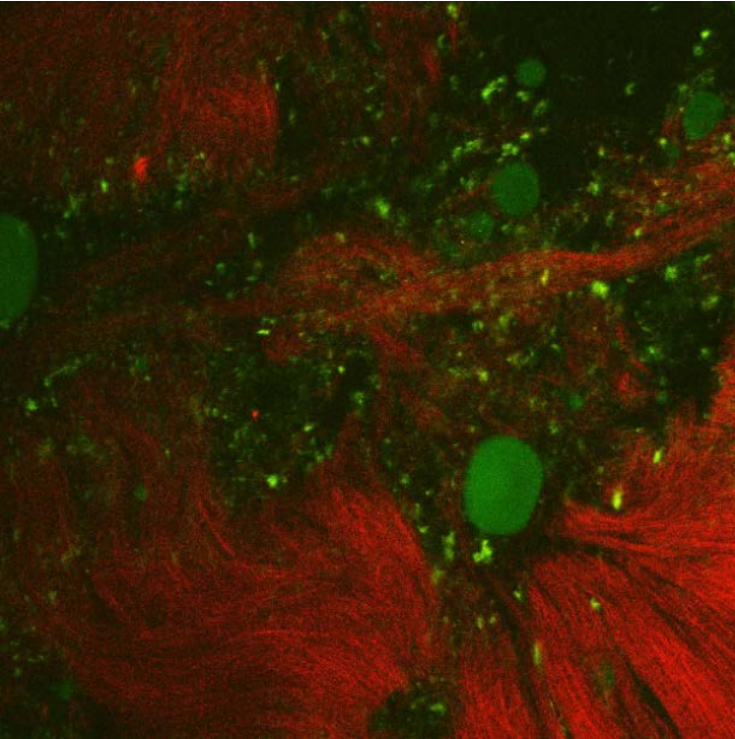
MPI of Au nanoparticles in water



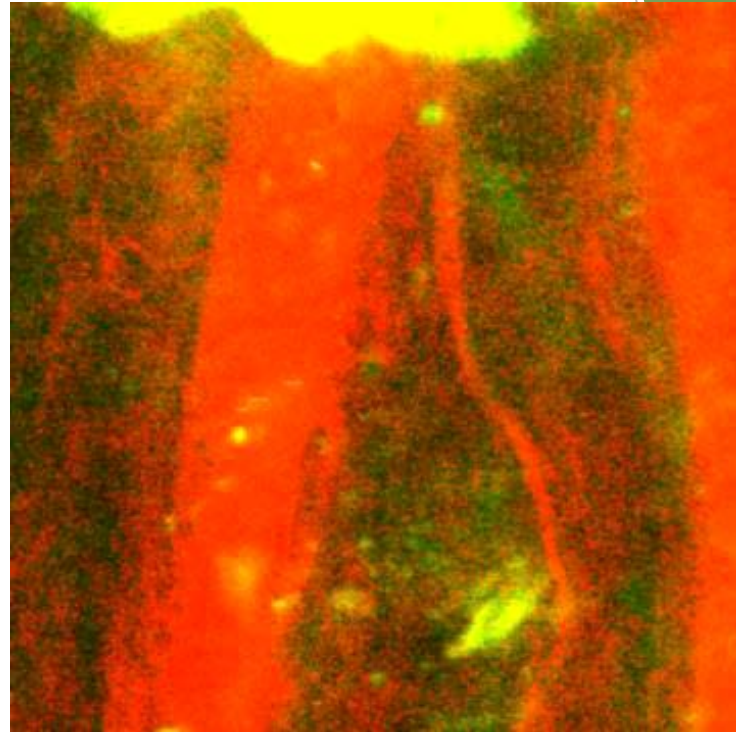
A Multiphoton imaging of GNPs in water with 5 mW (A) and 10 mW (B) 780 nm ti:sa laser irradiation. Red is SHG (registration range -380-400 nm) and green is TPF (430-650 nm).

Frame size 50 μm . Objective- 20 \times /NA 0.5.

MPI of Au nanorods in biotissues



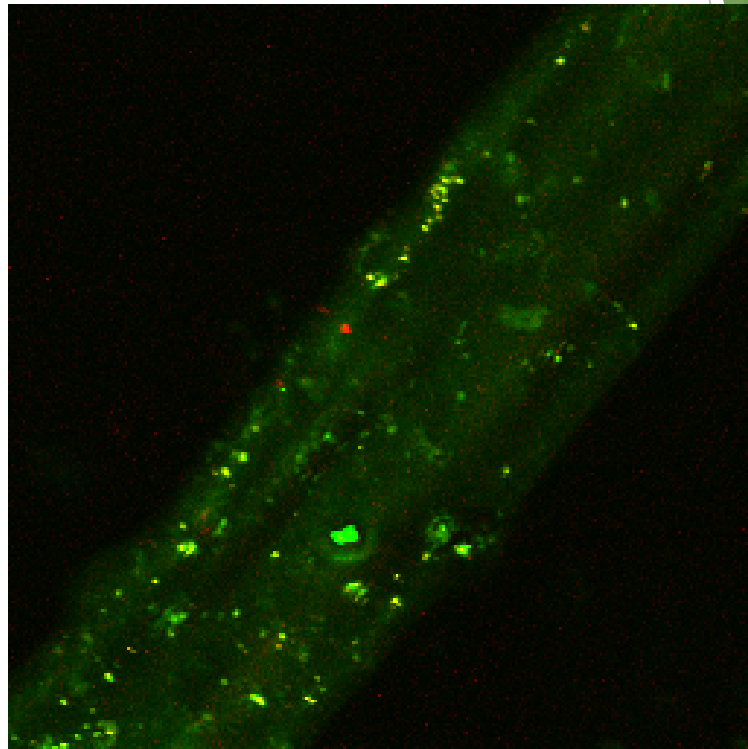
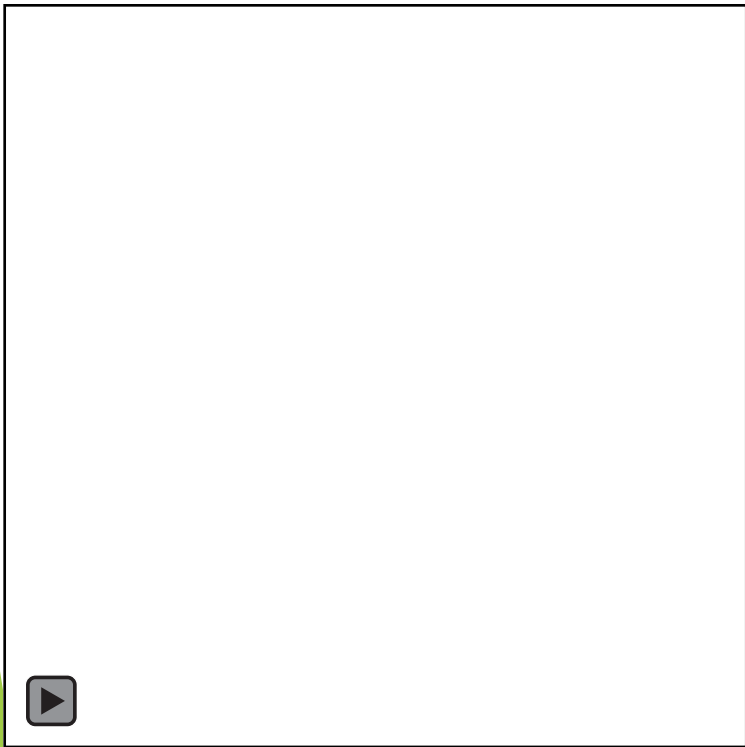
A



B

MPI of GNPs inside of a chicken skin. Irradiation intensity 8 mW (A) and 20 mW (B). SHG from collagen fibers also are seen as a red pseudocolor. Objective- 20×/NA 0.5.

MPI of Ag nanoparticles in water and biotissues

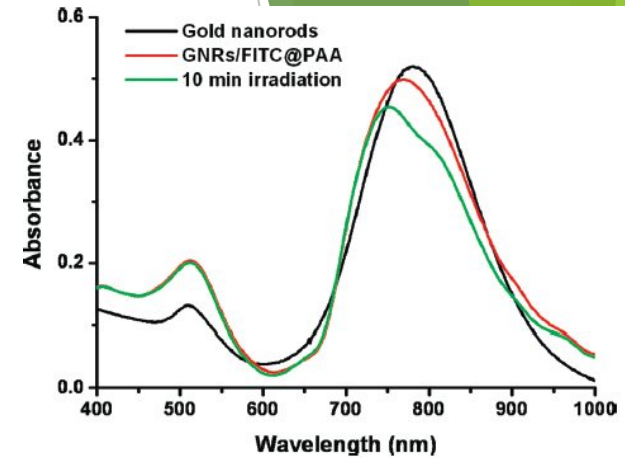
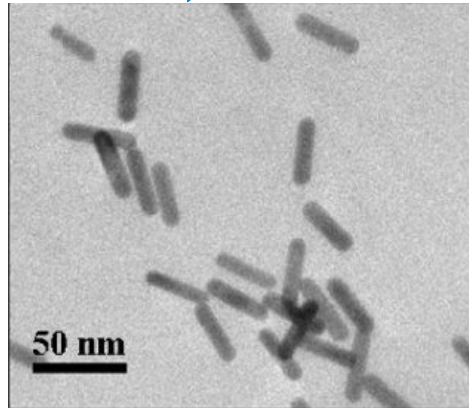
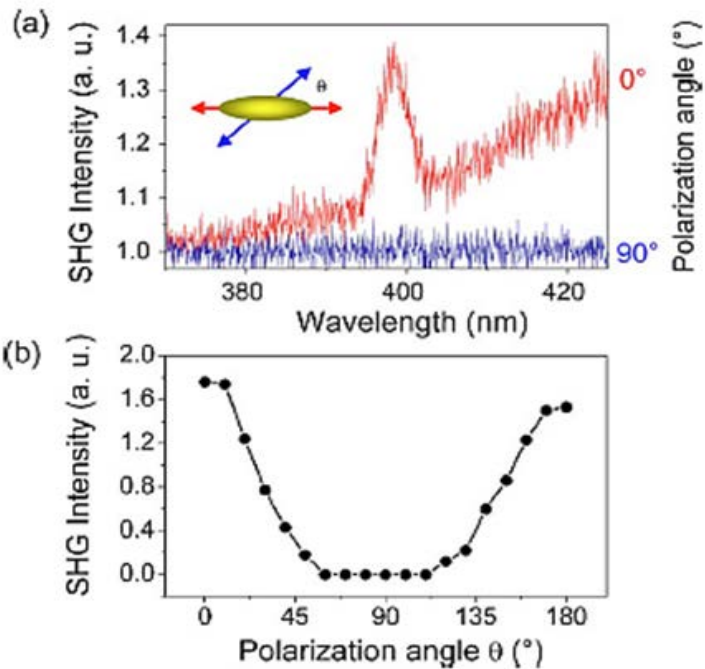


MPI of Ag nanoparticles near the edge of the water drop.
Frame size: $30 \times 30 \times 10 \mu\text{m}^3$

MPI of DNA fascicles in water+Ag NPs solution. Green (TPF), red (SHG) and yellow (TPF+SHG) spots in (B) indicate Ag nanoparticles or their aggregates.

Frame size $50 \times 0 \mu\text{m}^2$, $\lambda_{\text{exc}} = 760 \text{ nm}$.
Objective-40 \times /NA 1.2

Linear and nonlinear properties of gold nanorods (GNRs)



Polarization studies demonstrate **resonance enhancement of the SHG intensity from GNRs**. The maximal SHG signal is obtained when the incident light polarization direction is parallel to the nanorod long axis.

“Role of surface plasmon in second harmonic generation from gold nanorods,” C. Hubert, L. Billot, P.-M. Adam, et al. *APL*. **90**, 181105. (2007)

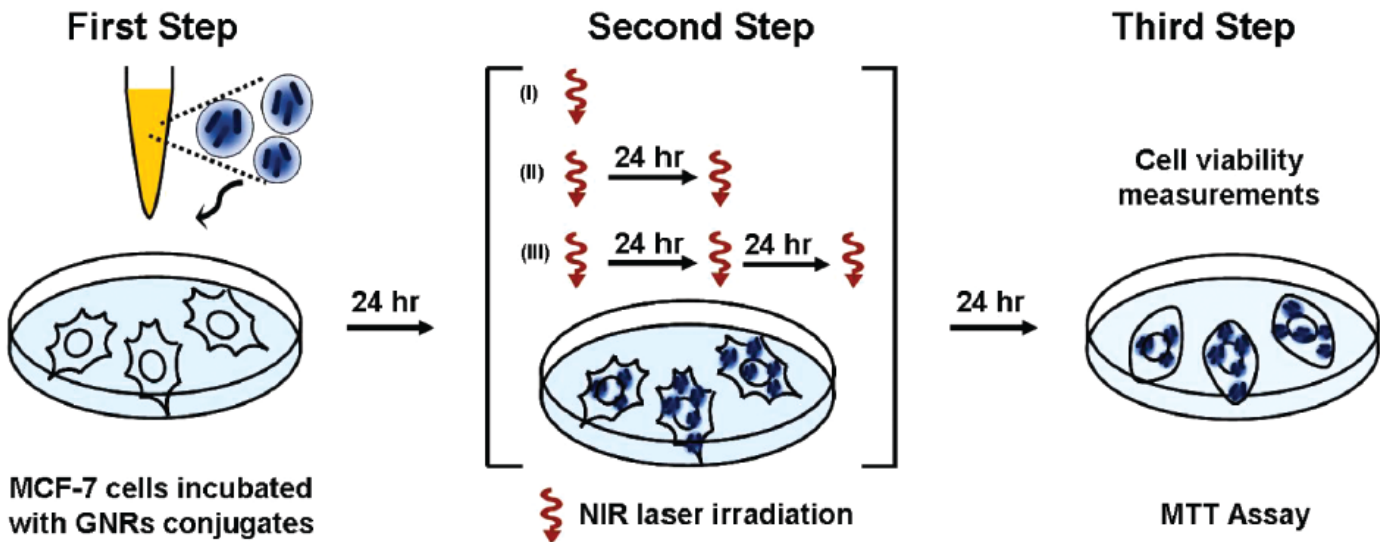
TEM images of GNR used in the research

Absorption spectra of GNR before and after irradiation with NIR FS laser for 10 min and GNRs/FITC@PAA conjugates.

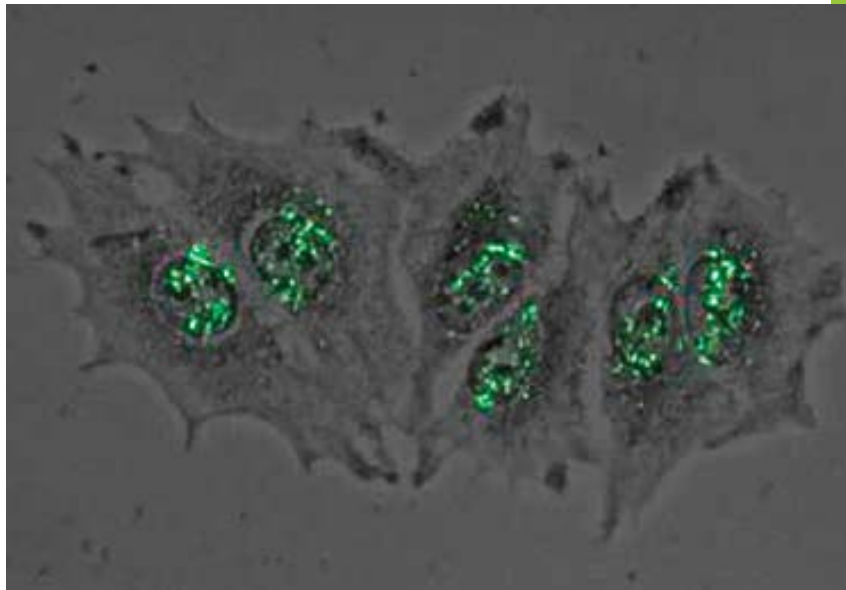
“Multiple release kinetics of targeted drug from gold nanorod embedded polyelectrolyte conjugates induced by NIR laser irradiation” TR Kuo, VA Hovhannisyan, YC Chao, et al. *J. Am. Chem. Soc.*, **132**, 14163(2010)

MPI of Au nanorods in cells

Experimental procedures to measure the cell viability of MCF-7 cells with GNR conjugates inside after laser irradiation.



Confocal microscopic image of MCF-7 cells incubated with GNRs@FITC/PAA conjugates (green color). The cross section image confirms that the conjugates are located inside the cells. Image size is $200 \times 140 \mu\text{m}^2$.



“Multiple release kinetics of targeted drug from gold nanorod embedded polyelectrolyte conjugates induced by NIR laser irradiation” TR Kuo, VA Hovhannisyanyan, YC Chao, et al. *J. Am. Chem. Soc.*, **132**, 14163 (2010)

Thanks for Your Attention!